Supporting Information

A method to predict binary eutectic mixtures for mechanochemical syntheses and cocrystallizations

Michele Prencipe[a,c], Paolo P. Mazzeo[a,b], Alessia Bacchi*[a,b,c]

[a] Department of Chemical Sciences, Life Sciences and Environmental Sustainability, University of Parma, Parco Area delle Scienze 17/A, 43124 Parma, Italy

[b] Biopharmanet-tec, Tecnopolo Padiglione 33, Campus Universitario, 43124 Parma, Italy

[c] CSGI: Center for Colloid and Surface Science, Via della Lastruccia 3 50019 - Sesto Fiorentino (FI), Italy

Email: alessia.bacchi@unipr.it

Differential Scanning Calorimetry

Differential Scanning Calorimetry data were collected on pure components and on the experimental sets (training, validation) of binary mixtures. Thermograms were recorded and elaborated using Pyris Software V12 (PerkinElmer). Endothermic and exothermic peaks were integrated and the resulting enthalpy values reported in J/g. A summary of thermal events is outlined in Table S1, for pure components, and Table S2, for binary mixtures. Binary mixtures of APY-THY, BP-THY, and IMZ-THY gave a liquid phase at 293 K therefore they were not analysed by DSC.

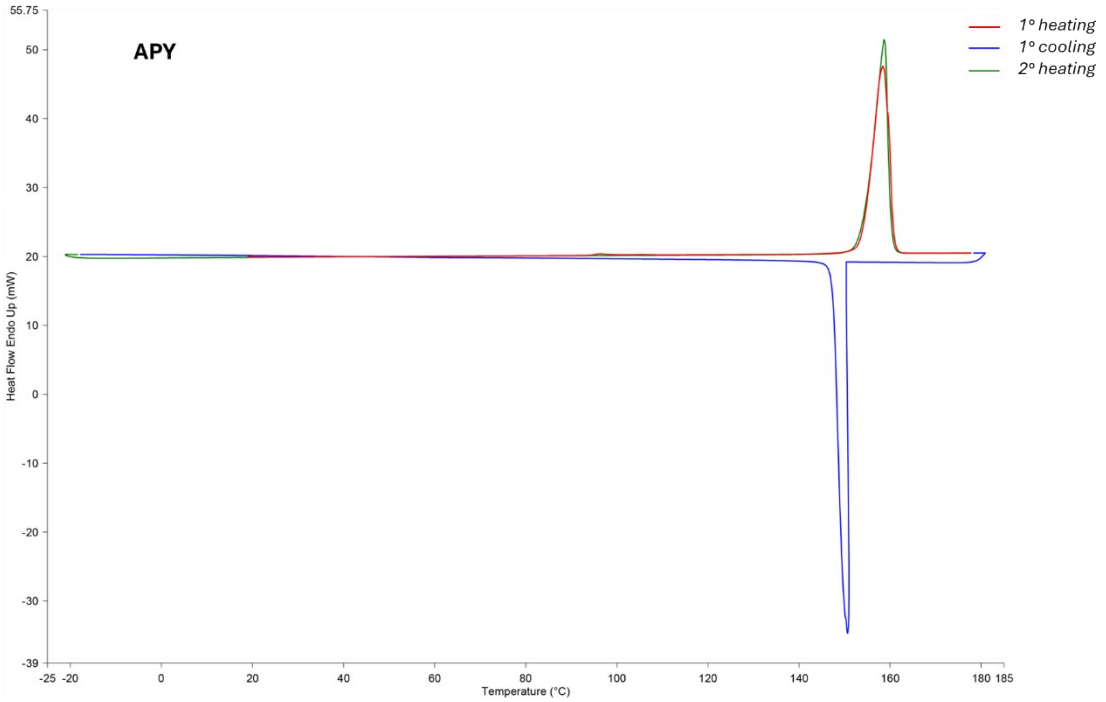

Figure S1. Thermogram of 4-aminopyridine (APY). First heating run from 20 °C to 180 °C (red curve), cooling run from 180 °C to -20 °C (blue curve) and second heating run from -20 °C to 180 °C (green curve). The whole firing profile was performed at 5°C/min. The first endothermic peak at 96.23 °C accounts for an enantiotropic transition towards a new polymorphic phase, that melted at 158.37 °C. In the cooling run, the exothermic peak refers to the recrystallization of the new polymorphic phase that afterwards melted in the second heating run.

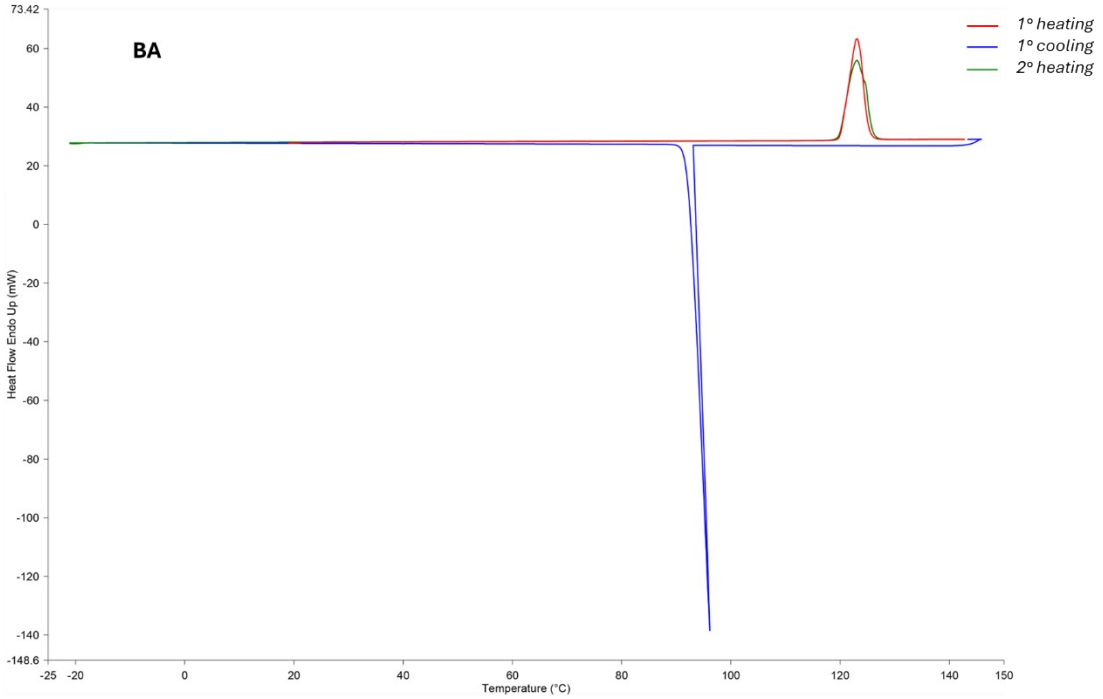

Figure S2. Thermogram of benzoic acid (BA). First heating run from 20 °C to 145 °C (red curve), cooling run from 145 °C to -20 °C (blue curve) and second heating run from -20 °C to 145 °C (green curve). The whole firing profile was performed at 5°C/min. The endothermic peaks shown in the heating runs refer to the melting of BA, while the exothermic peak in the cooling run refers to its recrystallization.

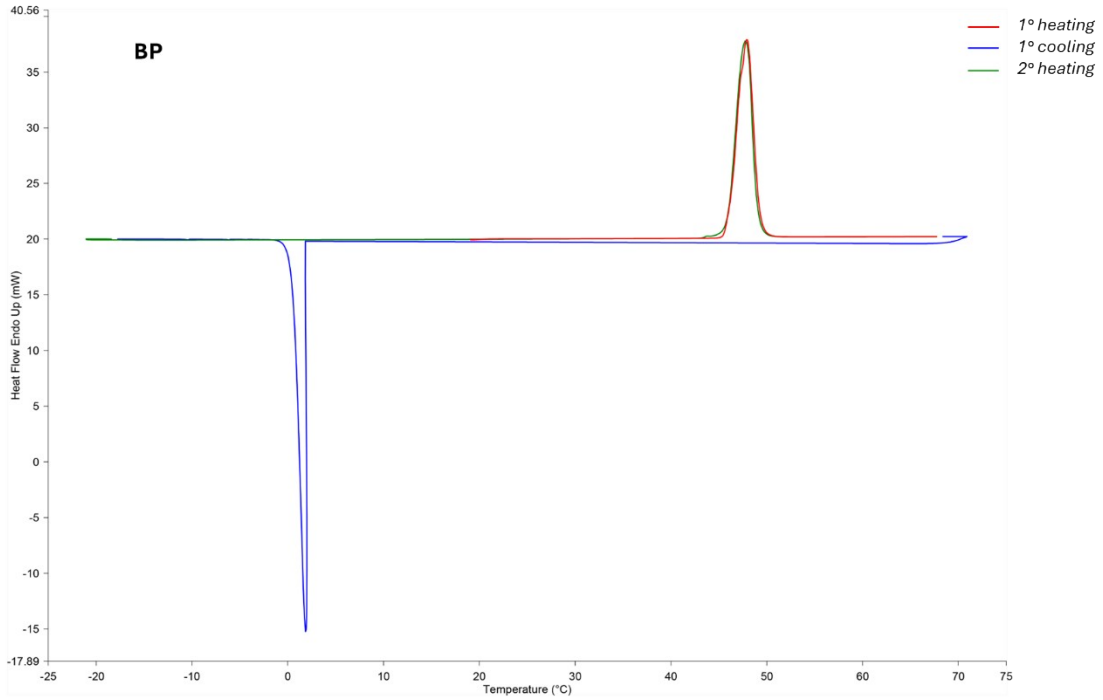

Figure S3. Thermogram of benzophenone (BP). First heating run from 20 °C to 70 °C (red curve), cooling run from 70 °C to -20 °C (blue curve) and second heating run from -20 °C to 70 °C (green curve). The whole firing profile was performed at 5°C/min. The endothermic peaks shown in the heating runs refer to the melting of BP, while the exothermic peak in the cooling run refers to its recrystallization.

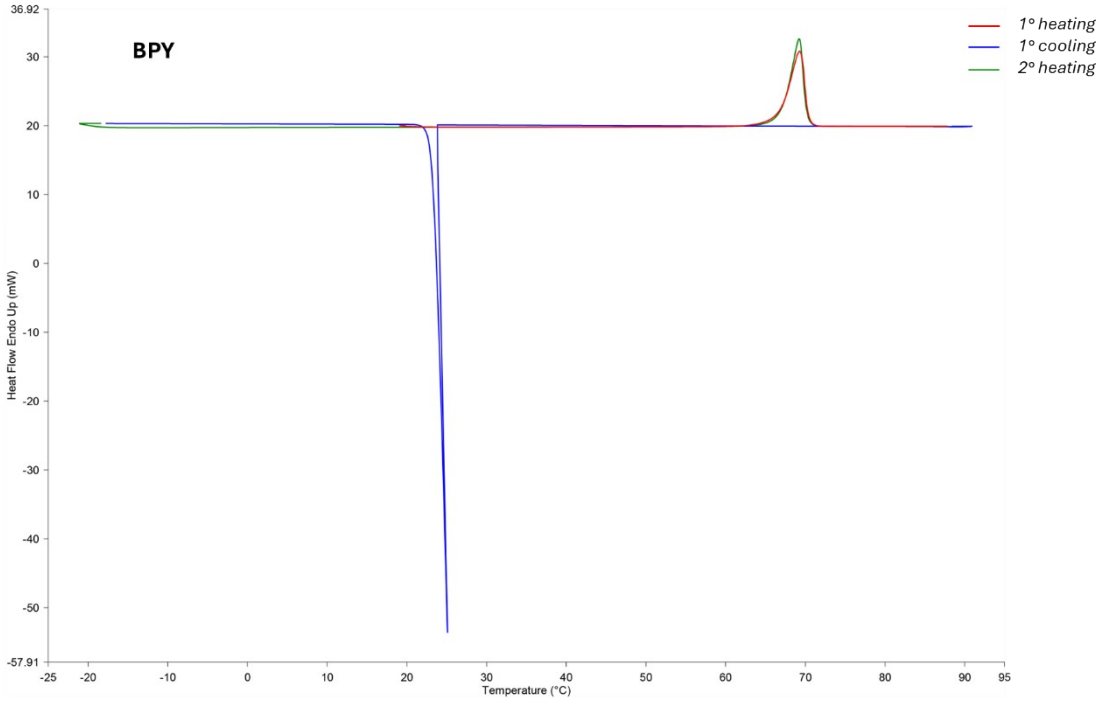

Figure S4. Thermogram of 2,2-bipyridine (BPY). First heating run from 20 °C to 90 °C (red curve), cooling run from 90 °C to -20 °C (blue curve) and second heating run from -20 °C to 90 °C (green curve). The whole firing profile was performed at 5°C/min. The endothermic peaks shown in the heating runs refer to the melting of BPY, while the exothermic peak in the cooling run refers to its recrystallization.

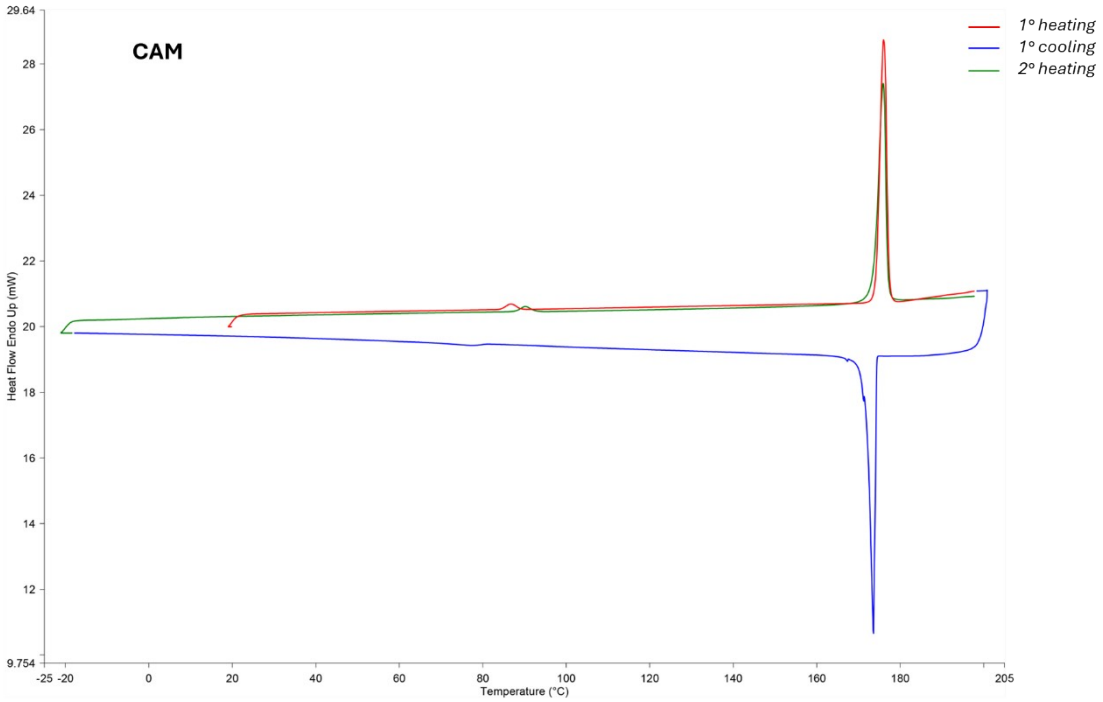

Figure S5. Thermogram of camphor (CAM). First heating run from 20 °C to 200 °C (red curve), cooling run from 200 °C to -20 °C (blue curve) and second heating run from -20 °C to 200 °C (green curve). The whole firing profile was performed at 5°C/min. The first endothermic peaks shown in the heating runs refer to an enantiotropic transition towards a polymorphic phase, that afterwards melts as confirmed by the endothermic peaks at 175.99 °C (1st heating) and 175.93 °C (2nd heating). The exothermic peak in the cooling run refers to the crystallization of the former phase.

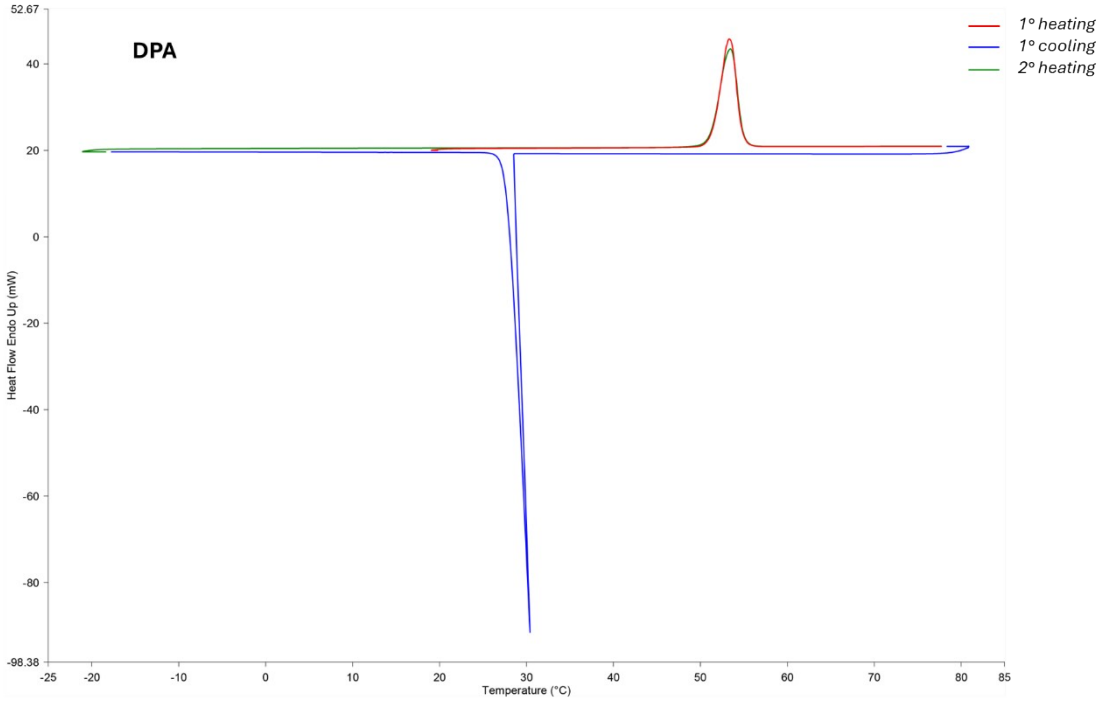

Figure S6. Thermogram of diphenylamine (DPA). First heating run from 20 °C to 80 °C (red curve), cooling run from 80 °C to -20 °C (blue curve) and second heating run from -20 °C to 80 °C (green curve). The whole firing profile was performed at 5°C/min. The endothermic peaks shown in the heating runs refer to the melting of DPA, while the exothermic peak in the cooling run refers to its recrystallization.

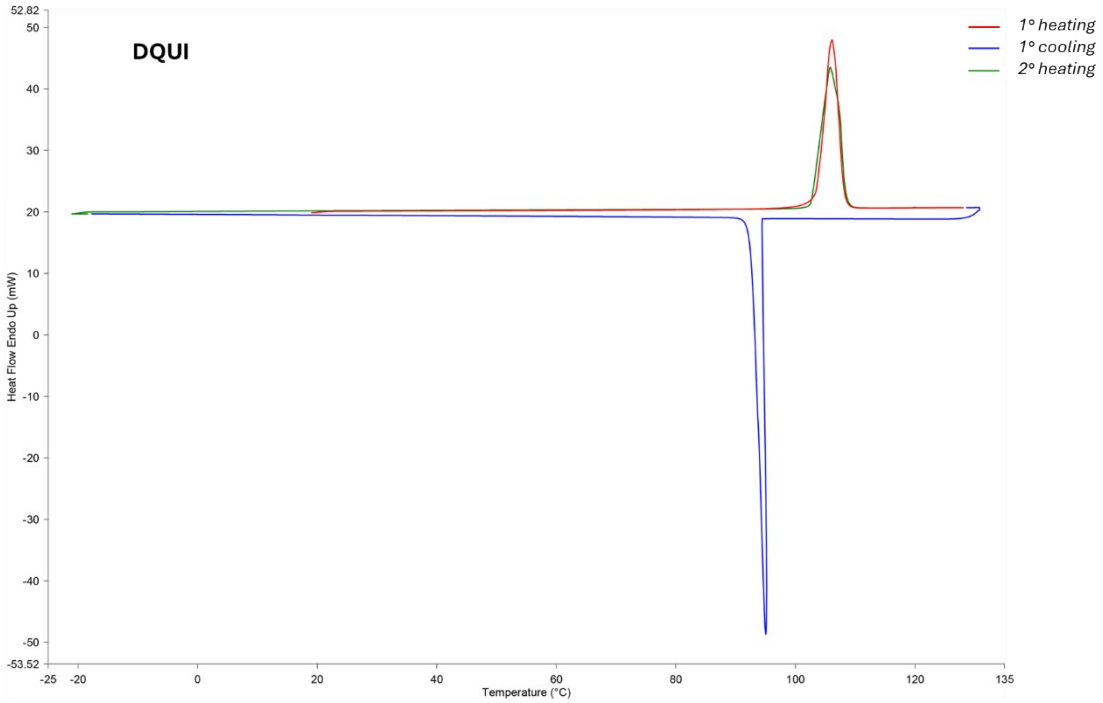

Figure S7. Thermogram of 2,3-dimethylquinoxaline (DQUI). First heating run from 20 °C to 130 °C (red curve), cooling run from 130 °C to -20 °C (blue curve) and second heating run from -20 °C to 130 °C (green curve). The whole firing profile was performed at 5°C/min. The endothermic peaks shown in the heating runs refer to the melting of DQUI, while the exothermic peak in the cooling run refers to its recrystallization.

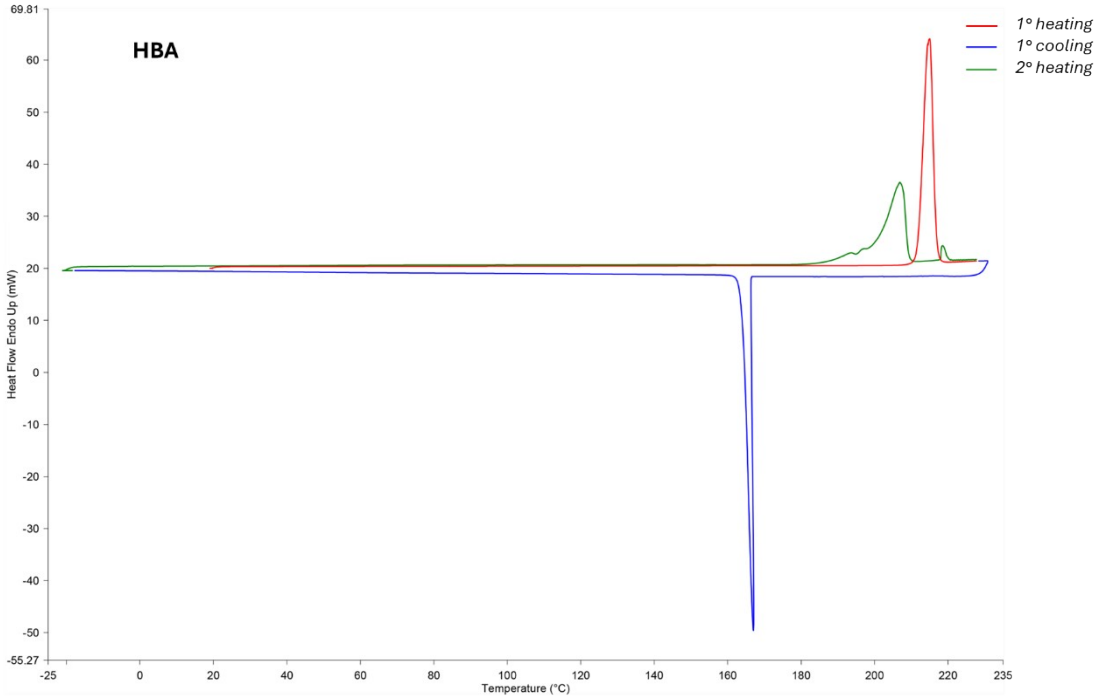

Figure S8. Thermogram of 4-hydroxybenzoic acid (HBA). First heating run from 20 °C to 230 °C (red curve), cooling run from 230 °C to -20 °C (blue curve) and second heating run from -20 °C to 230 °C (green curve). The whole firing profile was performed at 5°C/min. The endothermic peak shown in the first heating run refers to the melting of HBA, while the exothermic peak in the cooling run refers to the crystallization of a polymorphic phase, that melted in the second heating run.

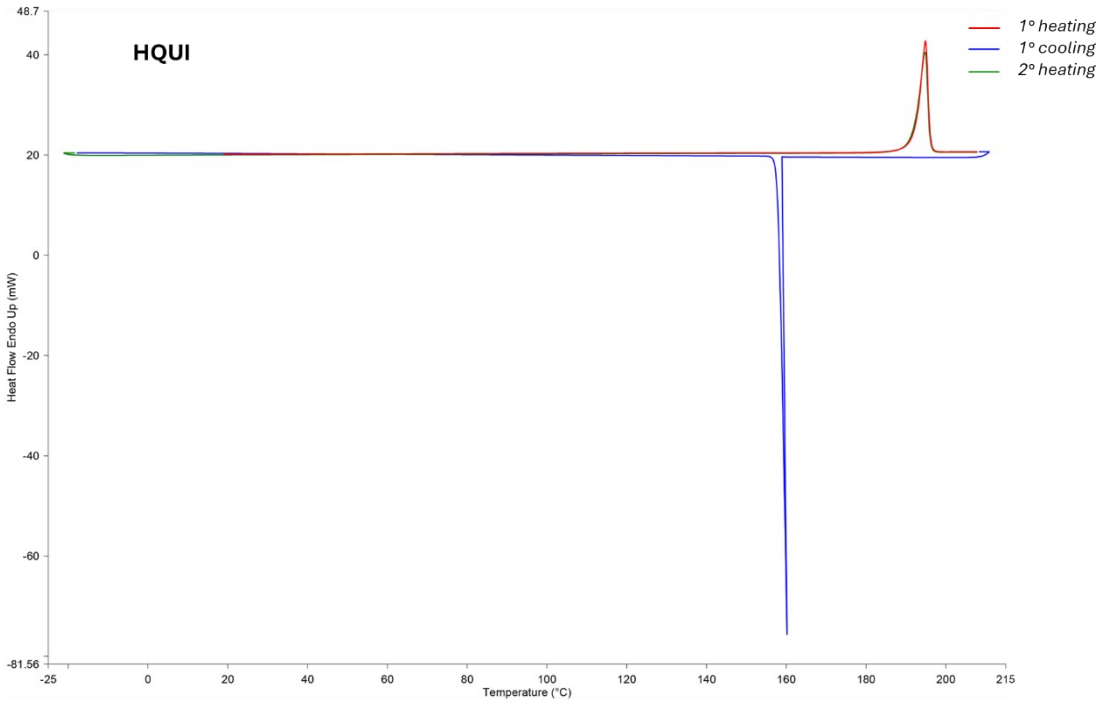

Figure S9. Thermogram of 6-hydroxyquinoline (HQUI). First heating run from 20 °C to 210 °C (red curve), cooling run from 210 °C to -20 °C (blue curve) and second heating run from -20 °C to 210 °C (green curve). The whole firing profile was performed at 5°C/min. The endothermic peaks shown in the heating runs refer to the melting of HQUI, while the exothermic peak in the cooling run refers to its recrystallization.

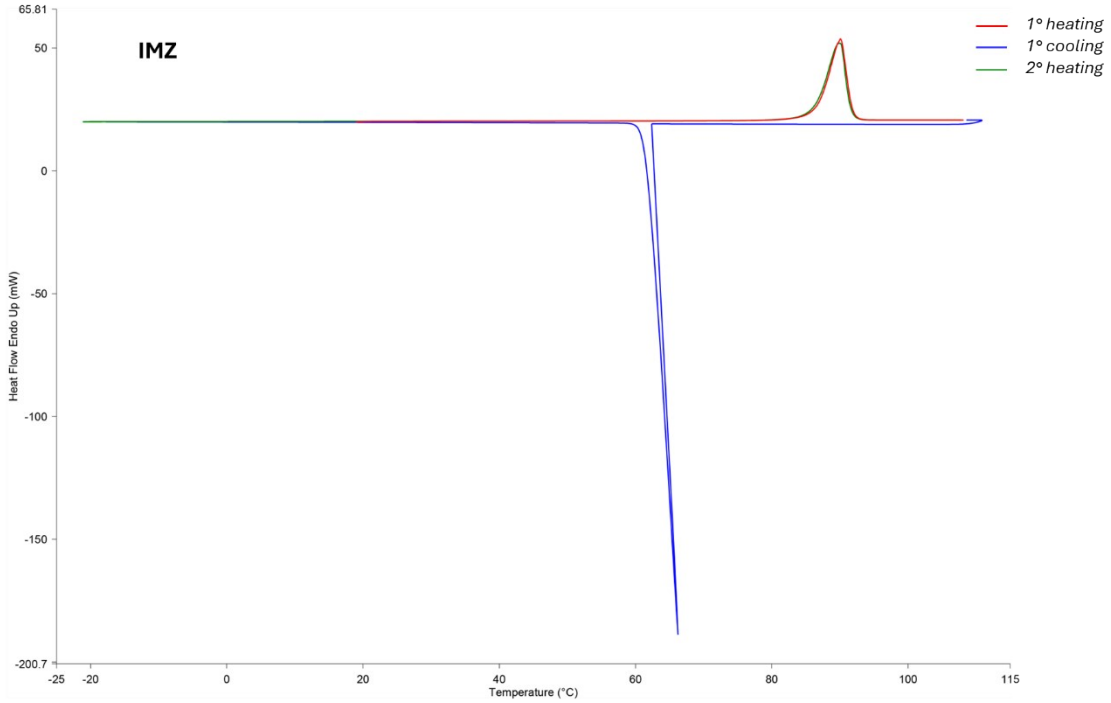

Figure S10. Thermogram of imidazole (IMZ). First heating run from 20 °C to 110 °C (red curve), cooling run from 110 °C to -20 °C (blue curve) and second heating run from -20 °C to 110 °C (green curve). The whole firing profile was performed at 5°C/min. The endothermic peaks shown in the heating runs refer to the melting of IMZ, while the exothermic peak in the cooling run refers to its recrystallization.

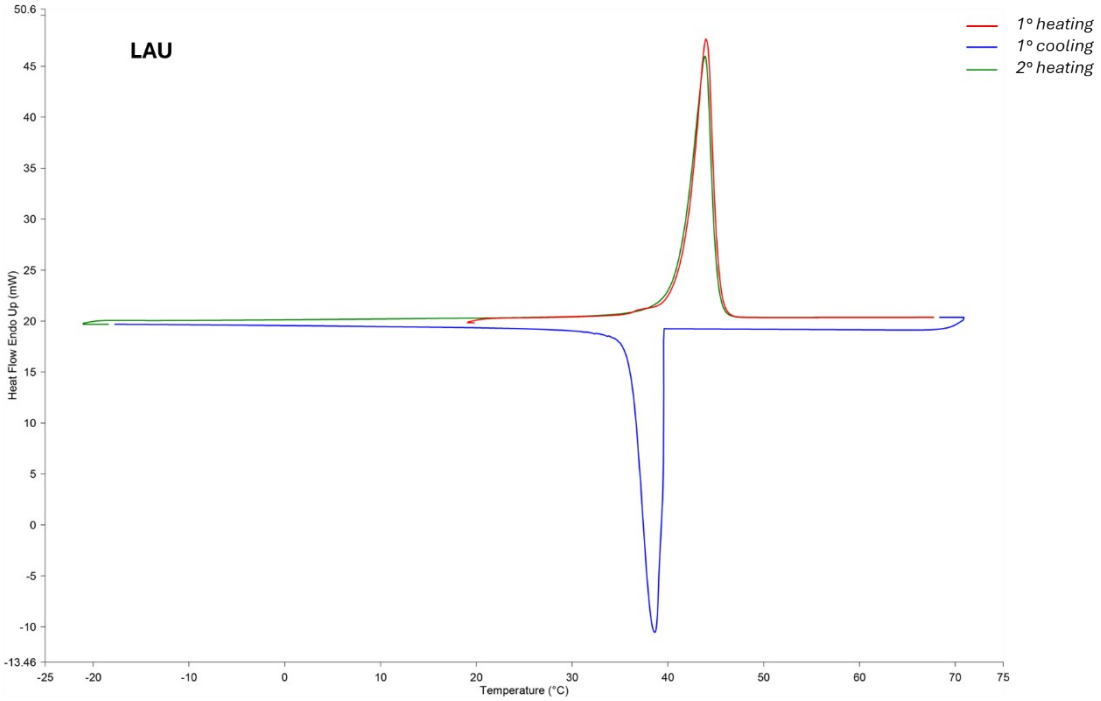

Figure S11. Thermogram of lauric acid (LAU). First heating run from 20 °C to 70 °C (red curve), cooling run from 70 °C to -20 °C (blue curve) and second heating run from -20 °C to 70 °C (green curve). The whole firing profile was performed at 5°C/min. The endothermic peaks shown in the heating runs refer to the melting of LAU, while the exothermic peak in the cooling run refers to its recrystallization.

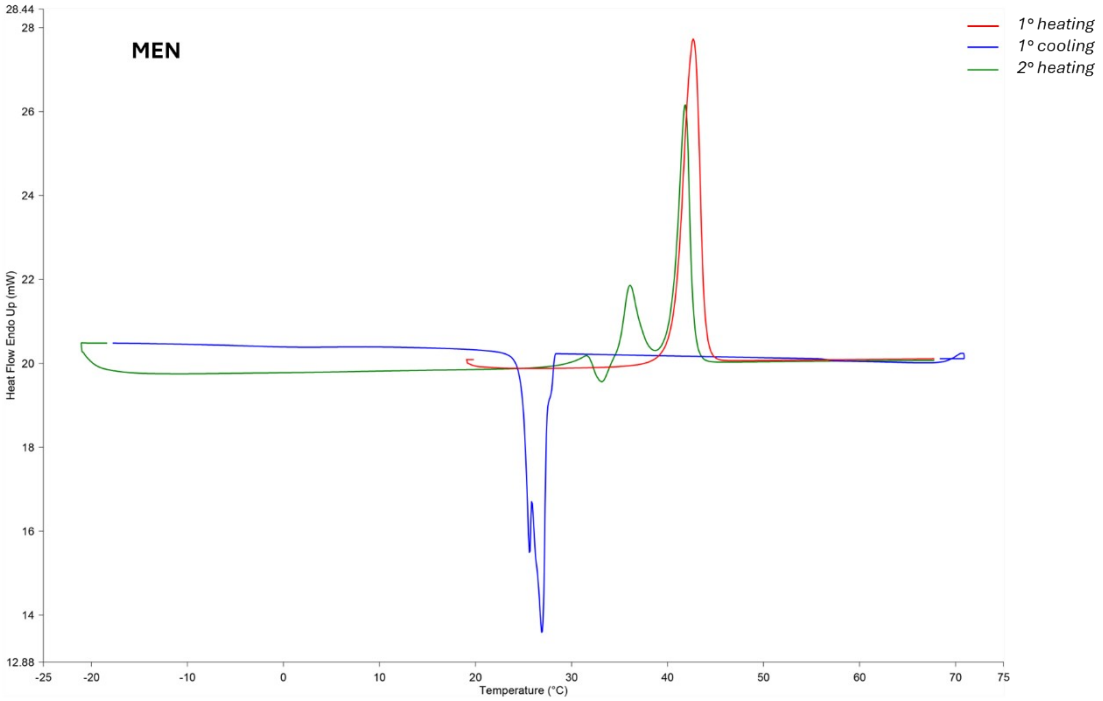

Figure S12. Thermogram of menthol (MEN). First heating run from 20 °C to 70 °C (red curve), cooling run from 70 °C to -20 °C (blue curve) and second heating run from -20 °C to 70 °C (green curve). The whole firing profile was performed at 5°C/min. The endothermic peak shown in the heating run refer to the melting of MEN, while the exothermic peak in the cooling run refers to the crystallization of a new polymorphic case. This is supported by the presence of a first endothermic peak in the second heating run at lower temperature (36.12 °C) due to the melting of the novel phase, in concomitance of the crystallization of the former phase at 33.16 °C, that afterwards melts at 41.87 °C.

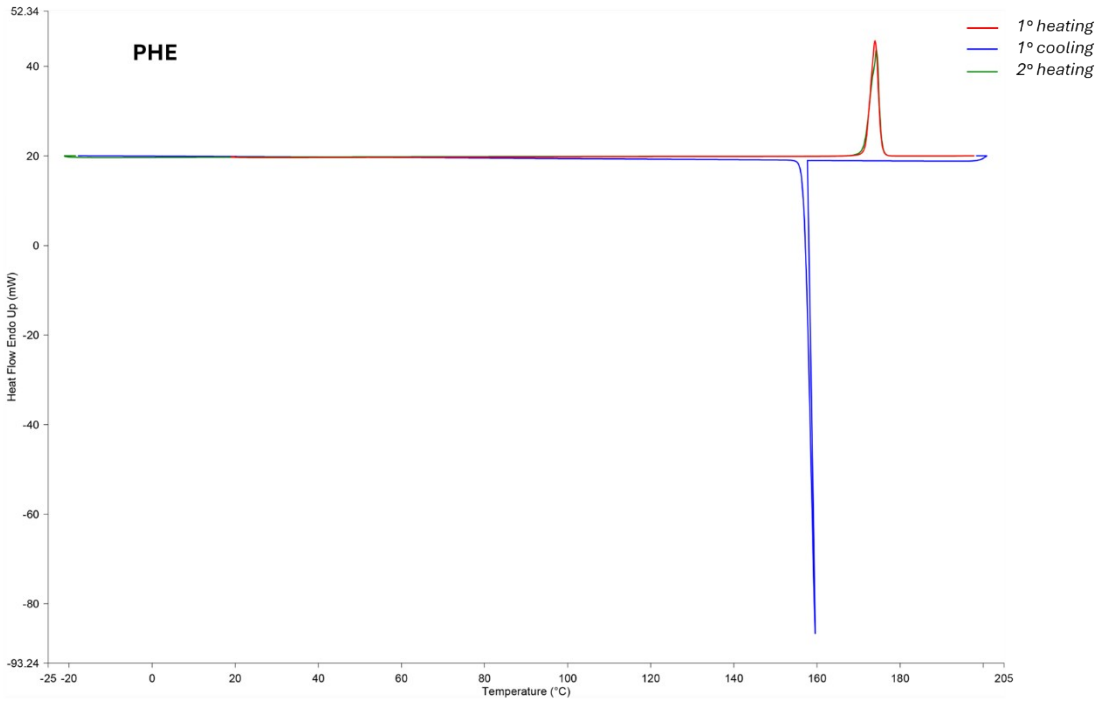

Figure S13. Thermogram of phenazine (PHE). First heating run from 20 °C to 200 °C (red curve), cooling run from 200 °C to -20 °C (blue curve) and second heating run from -20 °C to 200 °C (green curve). The whole firing profile was

performed at 5°C/min. The endothermic peaks shown in the heating runs refer to the melting of PHE, while the exothermic peak in the cooling run refers to its recrystallization.

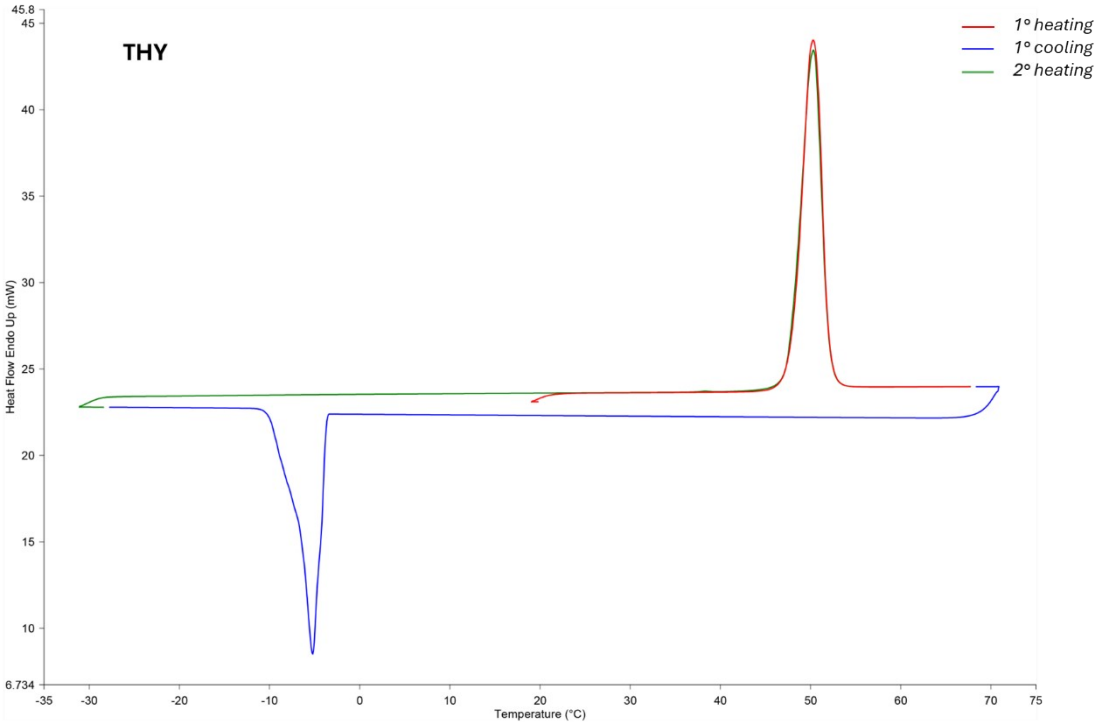

Figure S14. Thermogram of thymol (THY). First heating run from 20 °C to 70 °C (red curve), cooling run from 70 °C to -20 °C (blue curve) and second heating run from -20 °C to 70 °C (green curve). The whole firing profile was performed at 5°C/min. The endothermic peaks shown in the heating runs refer to the melting of THY, while the exothermic peak in the cooling run refers to its recrystallization.

Table S1. Summary of the thermal events that occurred during DSC measurements of pure components.

Component	*Run*		*Thermal event*	*Temperature (°C)*	*ΔH (J g^{-1})*
APY	First heating	1st peak	Endothermic	96.23	0.97
		2nd peak	Endothermic	158.37	209.89
	First cooling	1st peak	Exothermic	150.65	-208.73
	Second heating	1st peak	Endothermic	158.72	208.66
BA	First heating	1st peak	Endothermic	123.05	141.39
	First cooling	1st peak	Exothermic	96.14	-130.85
	Second heating	1st peak	Endothermic	123.11	139.40
BP**	First heating	1st peak	Endothermic	47.89	111.12
	First cooling	1st peak	Exothermic	1.87	-93.74
	Second heating	1st peak	Endothermic	47.81	110.38
BPY*	First heating	1st peak	Endothermic	69.28	132.67
	First cooling	1st peak	Exothermic	25.10	-113.04
	Second heating	1st peak	Endothermic	69.24	129.99
CAM*	First heating	1st peak	Endothermic	86.64	1.26
		2nd peak	Endothermic	175.99	42.10
	First cooling	1st peak	Exothermic	173.61	-39.65
	Second heating	1st peak	Endothermic	90.14	1.30
		2nd peak	Endothermic	175.93	40.31
DPA*	First heating	1st peak	Endothermic	55.33	121.60
	First cooling	1st peak	Exothermic	30.42	-110.74
	Second heating	1st peak	Endothermic	55.45	121.08
DQUI	First heating	1st peak	Endothermic	106.11	134.80
	First cooling	1st peak	Exothermic	95.02	-140.02
	Second heating	1st peak	Endothermic	105.87	141.33
HBA	First heating	1st peak	Endothermic	215.05	256.18
	First cooling	1st peak	Exothermic	167.03	-192.88
	Second heating	1st peak	Endothermic	206.92	211.06
		2nd peak	Endothermic	218.49	7.34
HQUI	First heating	1st peak	Endothermic	194.89	170.72
	First cooling	1st peak	Exothermic	160.20	-154.85
	Second heating	1st peak	Endothermic	194.76	167.42
IMZ	First heating	1st peak	Endothermic	90.09	185.17
	First cooling	1st peak	Exothermic	66.23	-180.95
	Second heating	1st peak	Endothermic	89.96	187.29
LAU*	First heating	1st peak	Endothermic	43.96	185.57
	First cooling	1st peak	Exothermic	38.61	-183.79
	Second heating	1st peak	Endothermic	43.90	183.90
MEN*	First heating	1st peak	Endothermic	42.68	91.85
	First cooling	1st peak	Exothermic	26.89	-67.51
	Second heating	1st peak	Endothermic	31.57	2.42
		2nd peak	Exothermic	33.16	-2.68
		3rd peak	Endothermic	36.12	17.09
		4th peak	Endothermic	41.87	49.97
PHE	First heating	1st peak	Endothermic	173.98	134.54
	First cooling	1st peak	Exothermic	159.57	-133.29
	Second heating	1st peak	Endothermic	174.28	135.61

*Component used only for PoEM's validation

**Component used both for training set and PoEM's validation

Table S1 Continued. Summary of the thermal events that occurred during DSC measurements of pure components.

Component	*Run*		*Thermal event*	*Temperature (°C)*	*ΔH (J g^{-1})*
PYR*	First heating	1st peak	Endothermic	27.37	9.26
		2nd peak	Endothermic	52.14	151.19
	First cooling	1st peak	Exothermic	42.62	-150.83
		2nd peak	Exothermic	20.04	-10.05
	Second heating	1st peak	Endothermic	20.38	10.87
		2nd peak	Endothermic	52.01	151.37
THY*	First heating	1st peak	Endothermic	50.33	119.57
	First cooling	1st peak	Exothermic	-5.20	-86.15
	Second heating	1st peak	Endothermic	50.33	117.32

*Component used only for PoEM's validation set

**Component used both for training set and PoEM's validation set

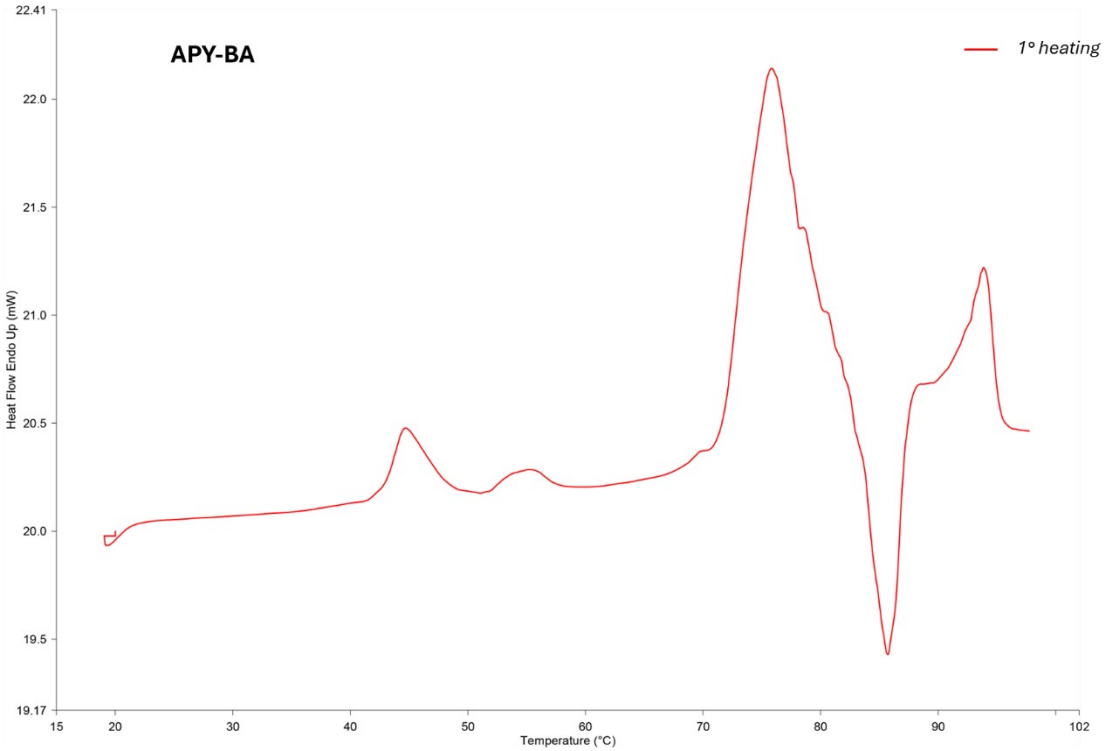

Figure S15. Thermogram of mixture APY-BA (χ_m(APY) = 0.3). Single heating run from 20 °C to 100 °C. The whole firing profile was performed at 5°C/min. The first endothermic peak (44.64 °C) refers to the melting of the eutectic mixture between APY and BA. A second endothermic peak was found at 55.07 °C, probably due to the melting of another eutectic mixture between a new unknown phase, formed in minor quantity during the mechanochemical mixing of components, and APY. The thermal behavior above 70°C is the result of multiple endothermic and exothermic events of difficult interpretation.

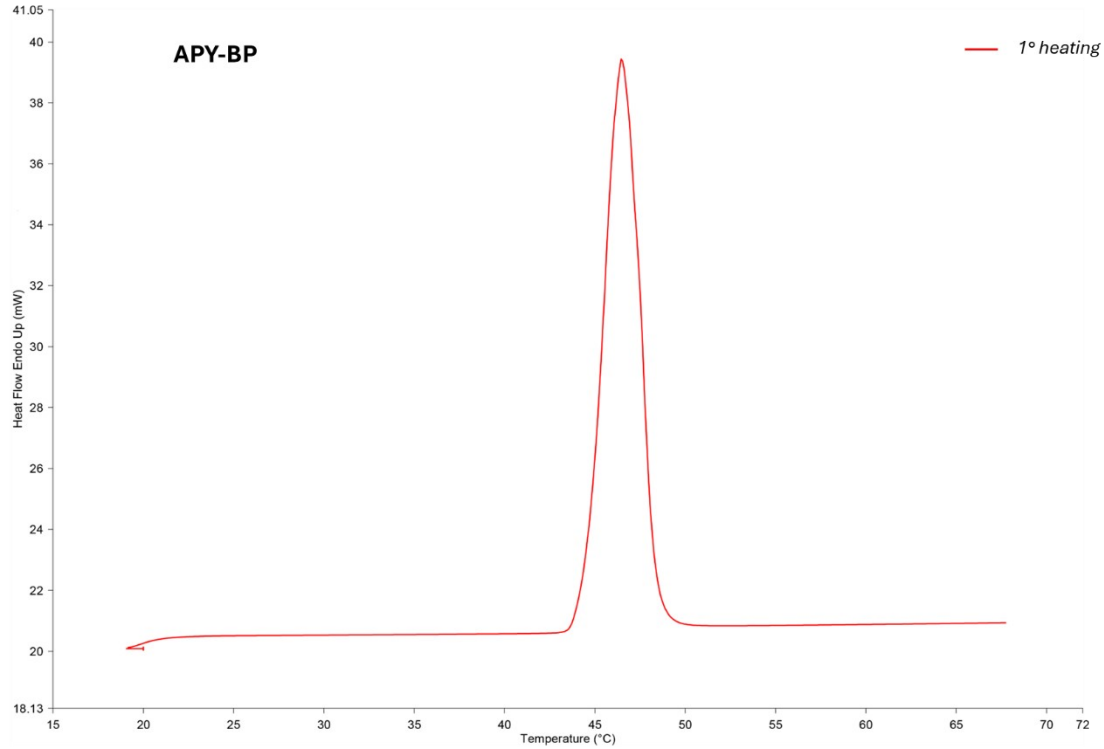

Figure S16. Thermogram of mixture APY-BP (χ_m(APY) = 0.2). Single heating run from 20 °C to 70 °C. The whole firing profile was performed at 5°C/min. The endothermic peak refers to the melting of the eutectic mixture between APY and BP.

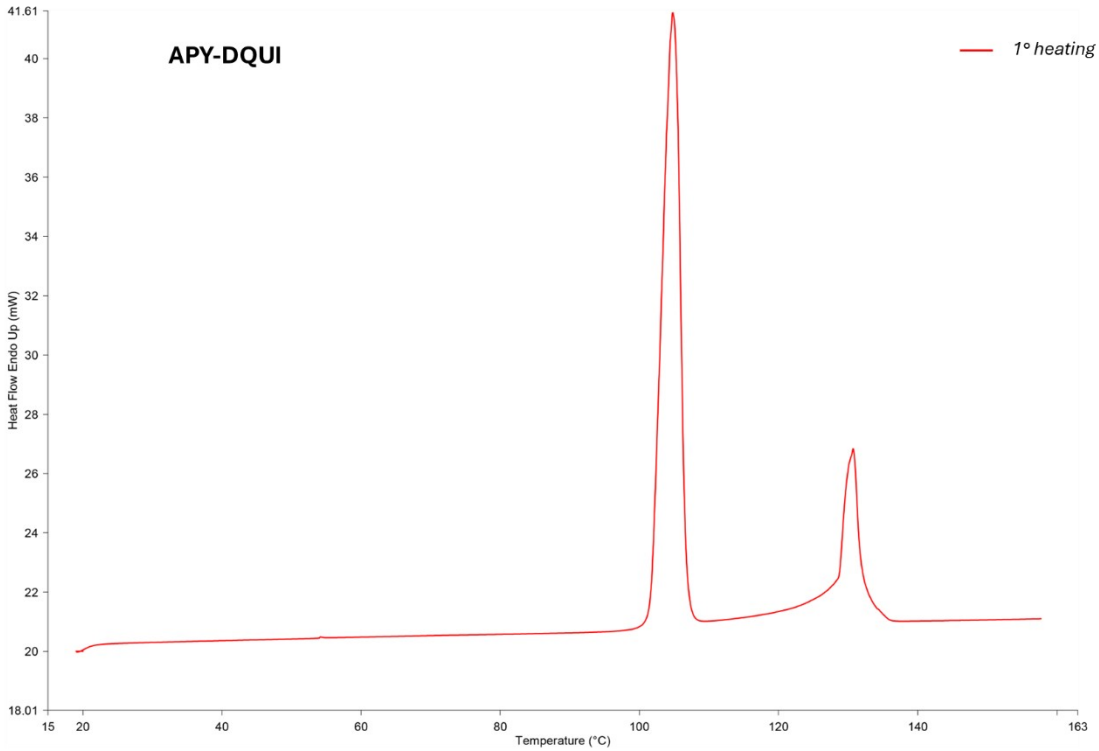

Figure S17. Thermogram of mixture APY-DQUI (χ_m(APY) = 0.3). Single heating run from 20 °C to 160 °C. The whole firing profile was performed at 5°C/min. The endothermic peak at 104.83 °C, refers to the melting of the eutectic mixture between APY and DQUI, followed by the melting of residual APY at 130.69 °C.

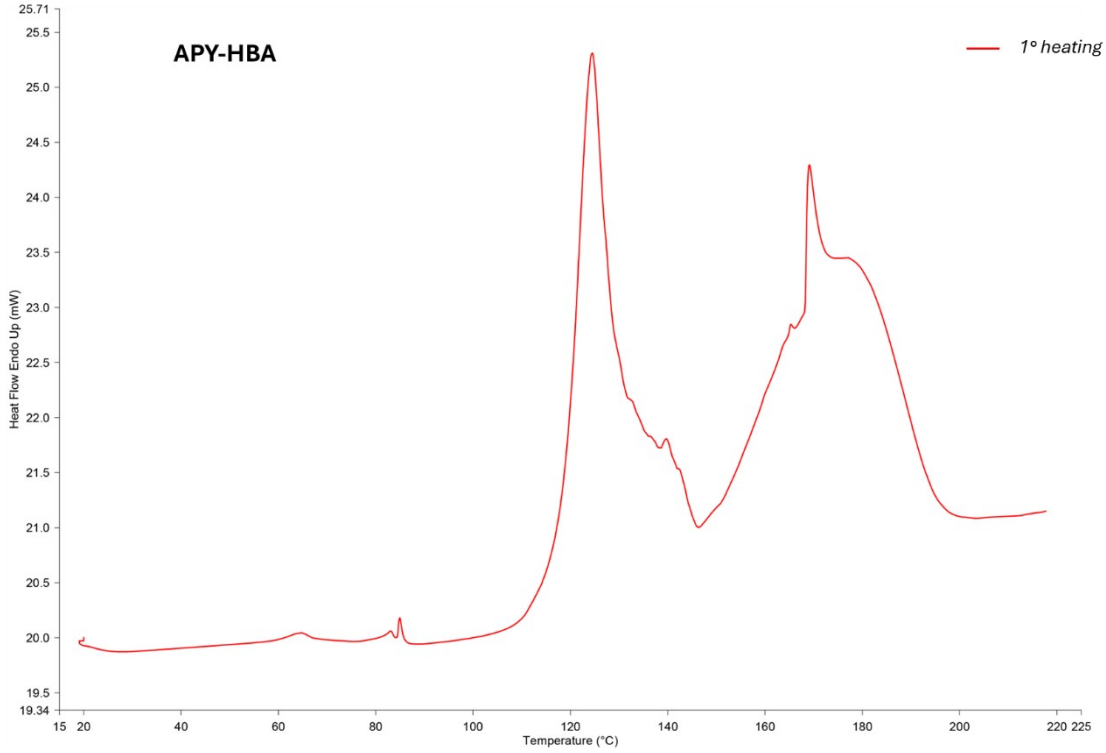

Figure S18. Thermogram of mixture APY-HBA (χ_m(APY) = 0.7). Single heating run from 20 °C to 220 °C. The whole firing profile was performed at 5°C/min. The endothermic peak at 124.55 °C refers to the melting of the eutectic mixture between APY and HBA, followed by the melting of residual HBA at 169.07 °C. The first endothermic peaks at 64.65 °C and 84.98 °C are of difficult interpretation.

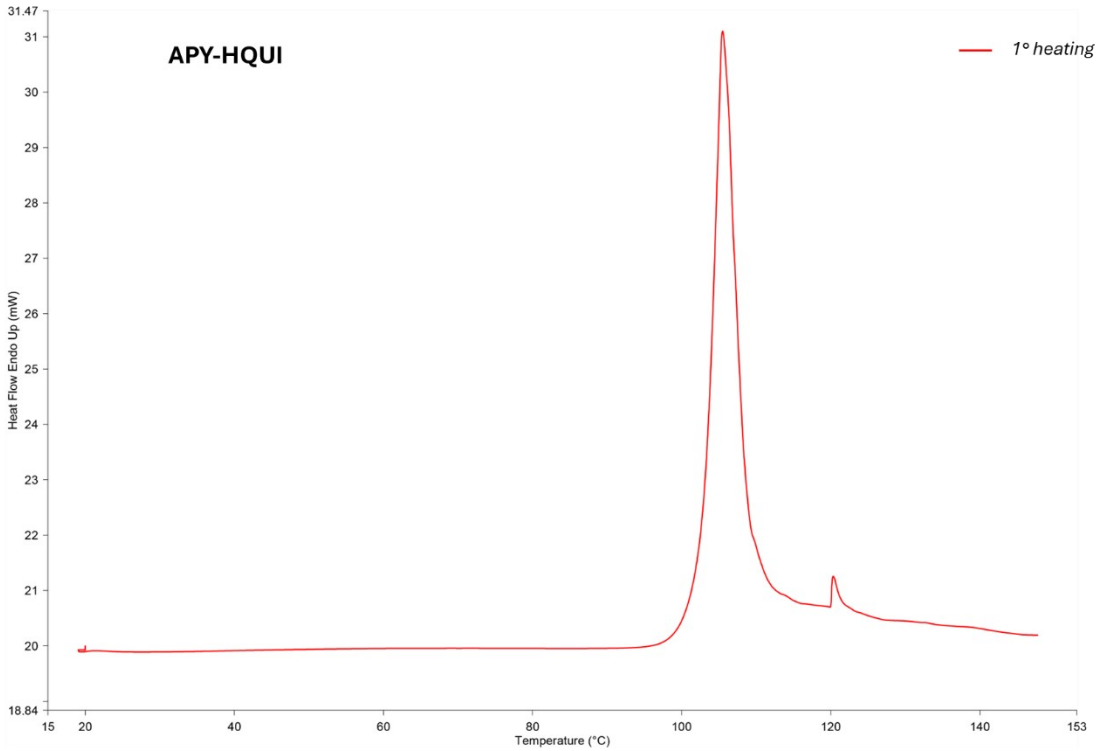

Figure S19. Thermogram of mixture APY-HQUI (χ_m(APY) = 0.7). Single heating run from 20 °C to 150 °C. The whole firing profile was performed at 5°C/min. The endothermic peak at 105.52 °C refers to the melting of the eutectic mixture between APY and HQUI, followed by the melting of residual APY at 120.38 °C.

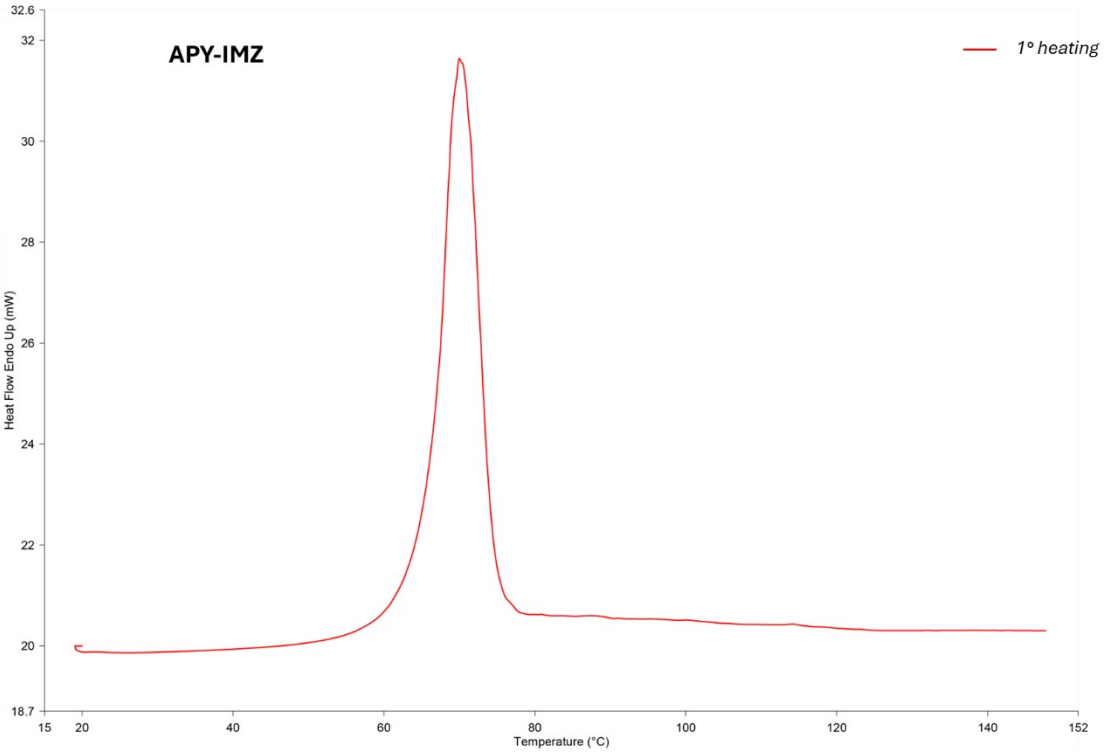

Figure S20. Thermogram of mixture APY-IMZ (χ_m(APY) = 0.3). Single heating run from 20 °C to 150 °C. The whole firing profile was performed at 5°C/min. The endothermic peak refers to the melting of the eutectic mixture between APY and IMZ.

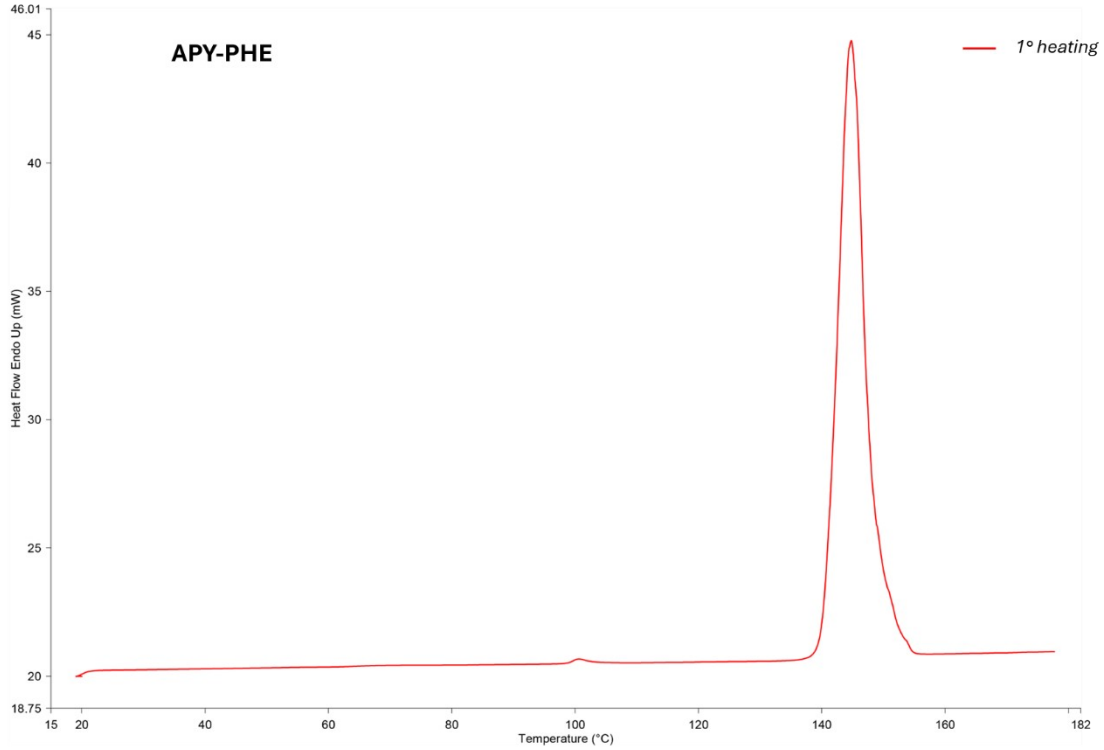

Figure S21. Thermogram of mixture APY-PHE (χ_m(APY) = 0.6). Single heating run from 20 °C to 180 °C. The whole firing profile was performed at 5°C/min. The endothermic peak refers to the melting of the eutectic mixture between APY and PHE.

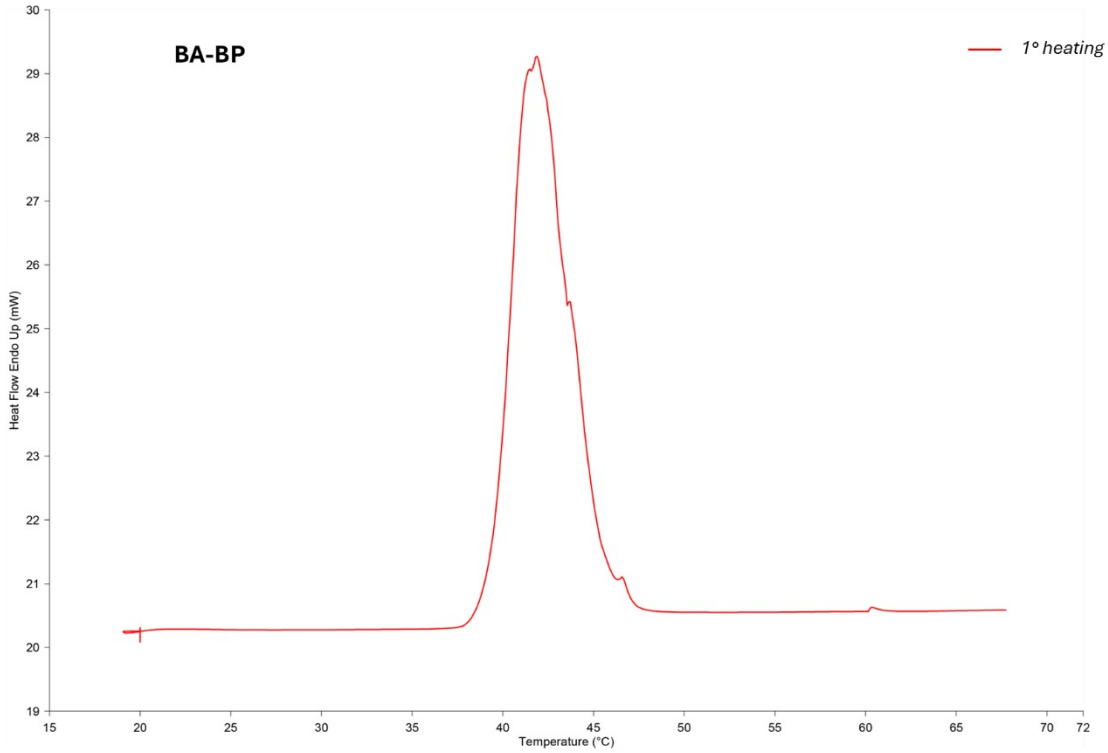

Figure S22. Thermogram of mixture BA-BP (χ_m(BA) = 0.3). Single heating run from 20 °C to 70 °C. The whole firing profile was performed at 5°C/min. The endothermic peak refers to the melting of the eutectic mixture between BA and BP.

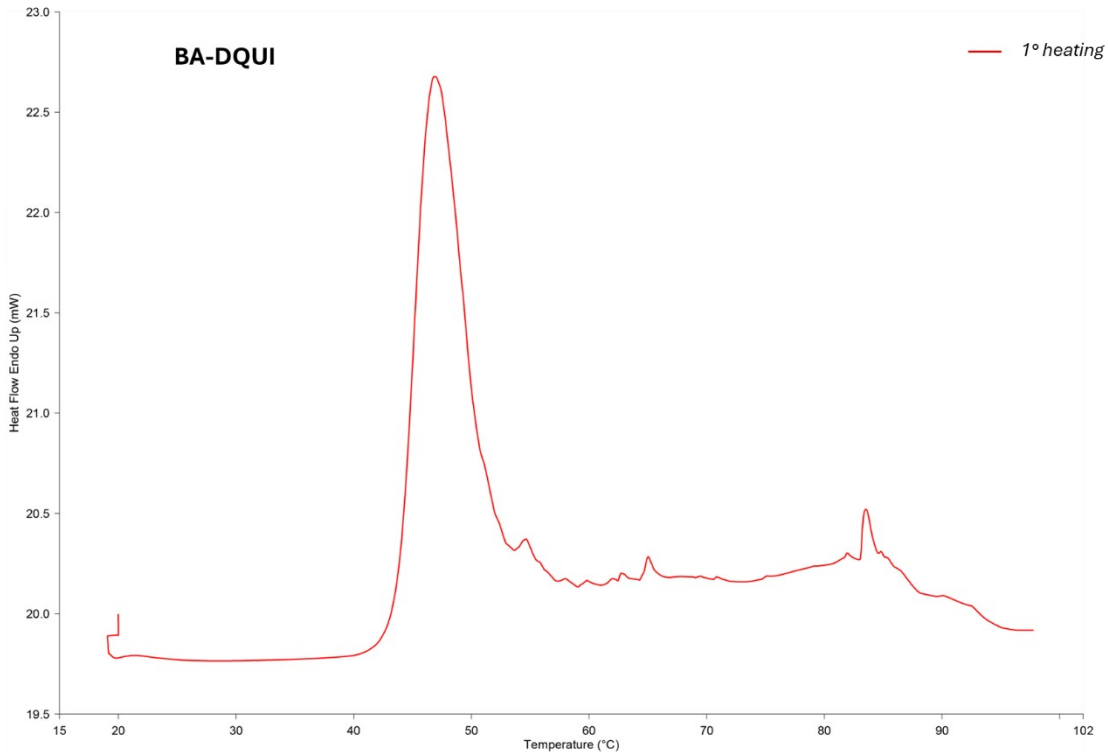

Figure S23. Thermogram of mixture BA-DQUI (χ_m(BA) = 0.4). Single heating run from 20 °C to 100 °C. The whole firing profile was performed at 5°C/min. The endothermic peak at 46.85°C refers to the melting of the eutectic mixture between BA and DQUI, followed by the melting of residual DQUI at 83.56 °C.

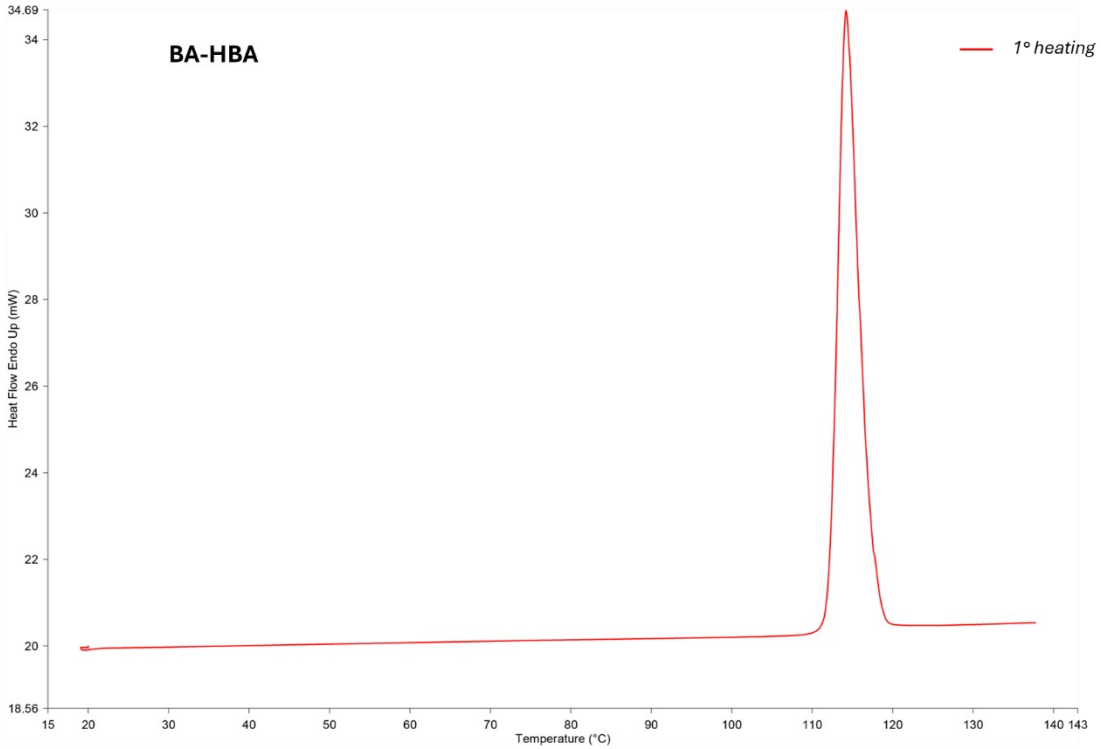

Figure S24. Thermogram of mixture BA-HBA (χ_m(BA) = 0.8). Single heating run from 20 °C to 140 °C. The whole firing profile was performed at 5°C/min. The endothermic peak refers to the melting of the eutectic mixture between BA and HBA.

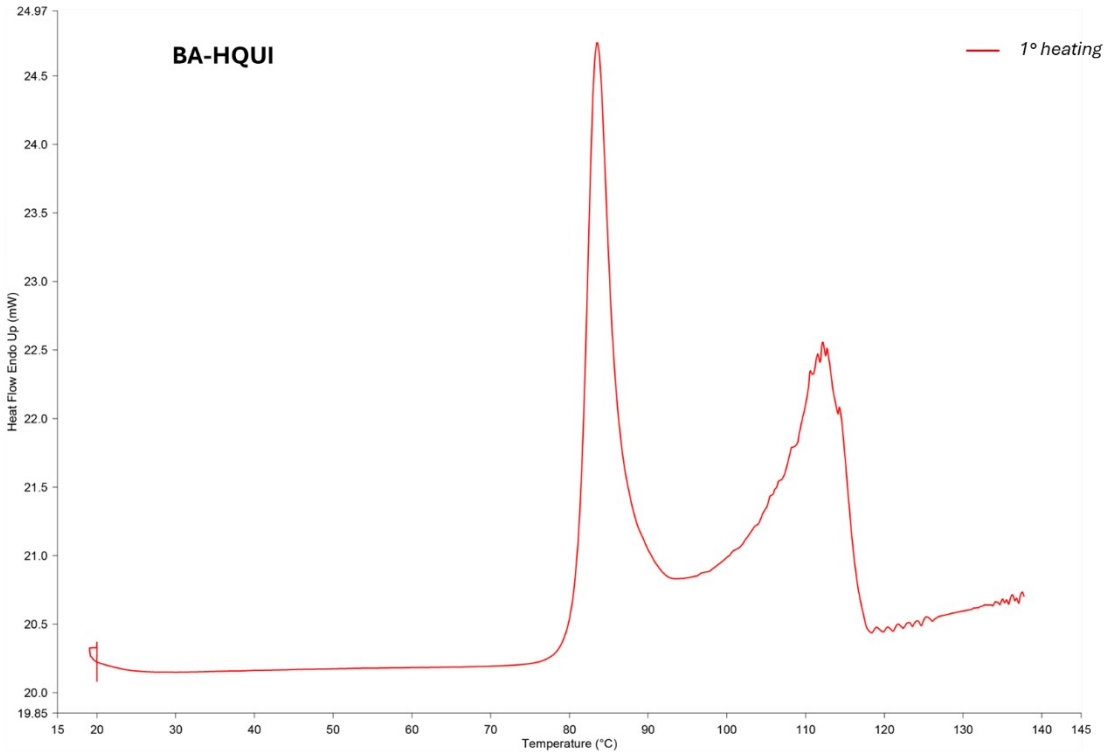

Figure S25. Thermogram of mixture BA-HQUI (χ_m(BA) = 0.8). Single heating run from 20 °C to 140 °C. The whole firing profile was performed at 5°C/min. The endothermic peak at 83.49°C refers to the melting of the eutectic mixture between BA and HQUI, followed by the melting of residual BA at 112.20 °C.

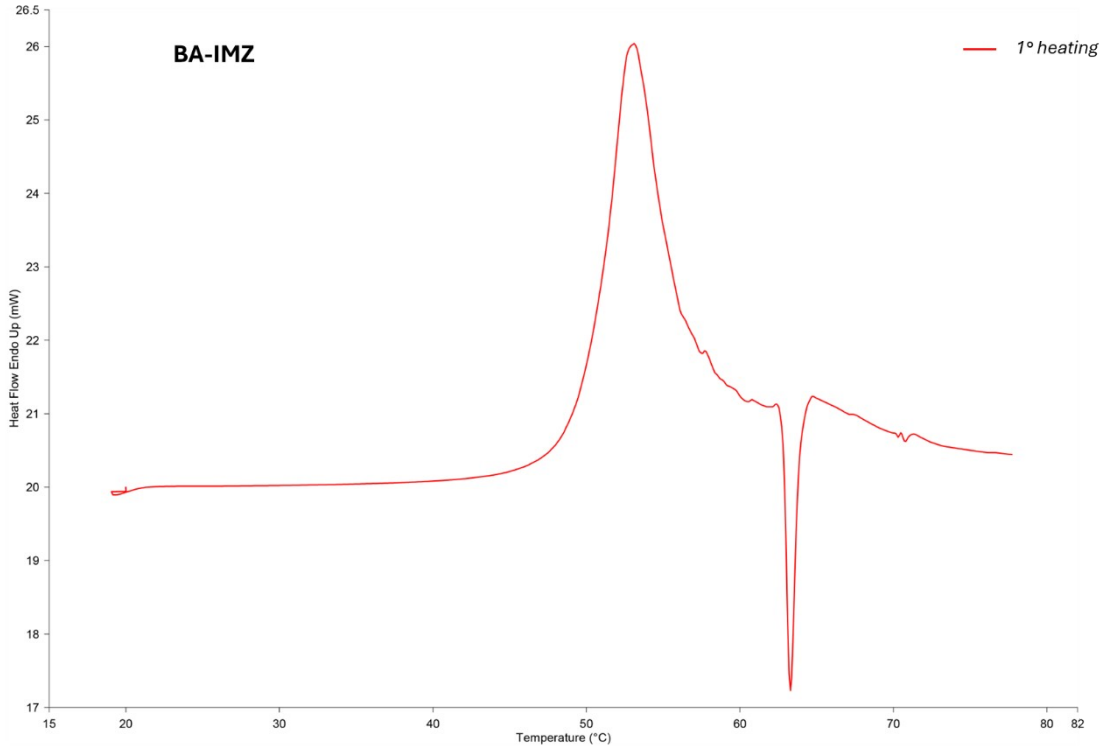

Figure S26. Thermogram of mixture BA-IMZ (χ_m(BA) = 0.3). Single heating run from 20 °C to 80 °C. The whole firing profile was performed at 5°C/min. The endothermic peak at 53.12 °C refers to the melting of the eutectic mixture between BA and IMZ, followed by an exothermic peak at 63.30 °C likely due to the crystallization of a new unknown phase.

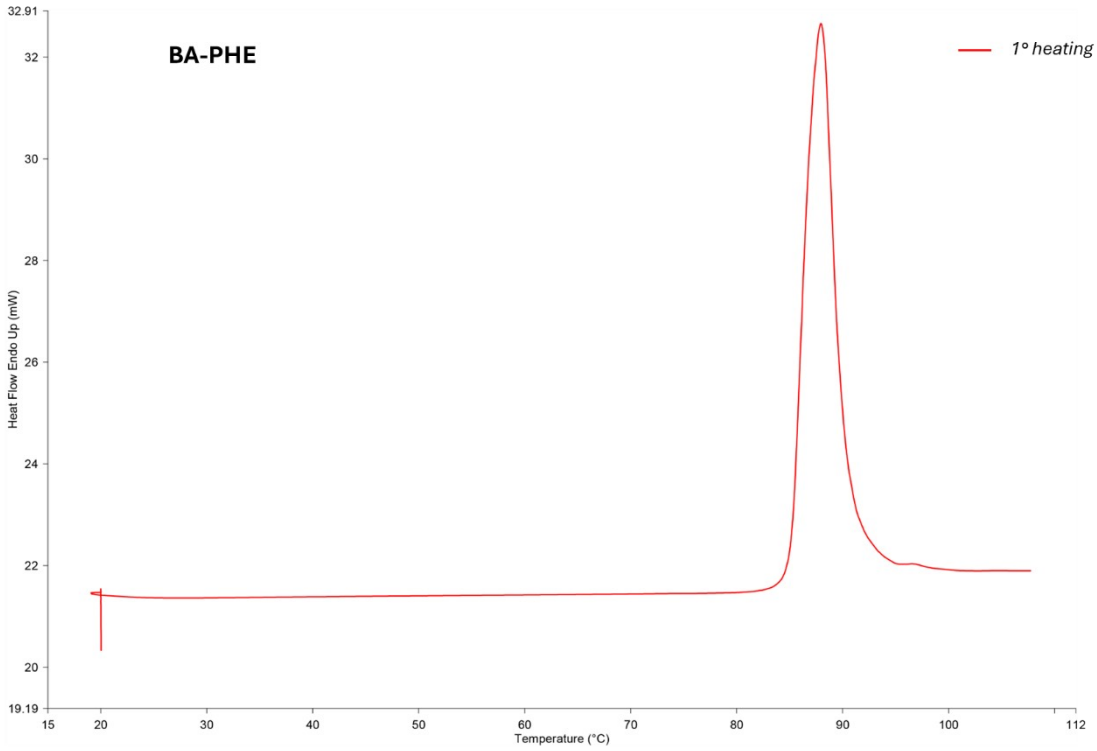

Figure S27. Thermogram of mixture BA-PHE (χ_m(BA) = 0.7). Single heating run from 20 °C to 110 °C. The whole firing profile was performed at 5°C/min. The endothermic peak refers to the melting of the eutectic mixture between BA and PHE.

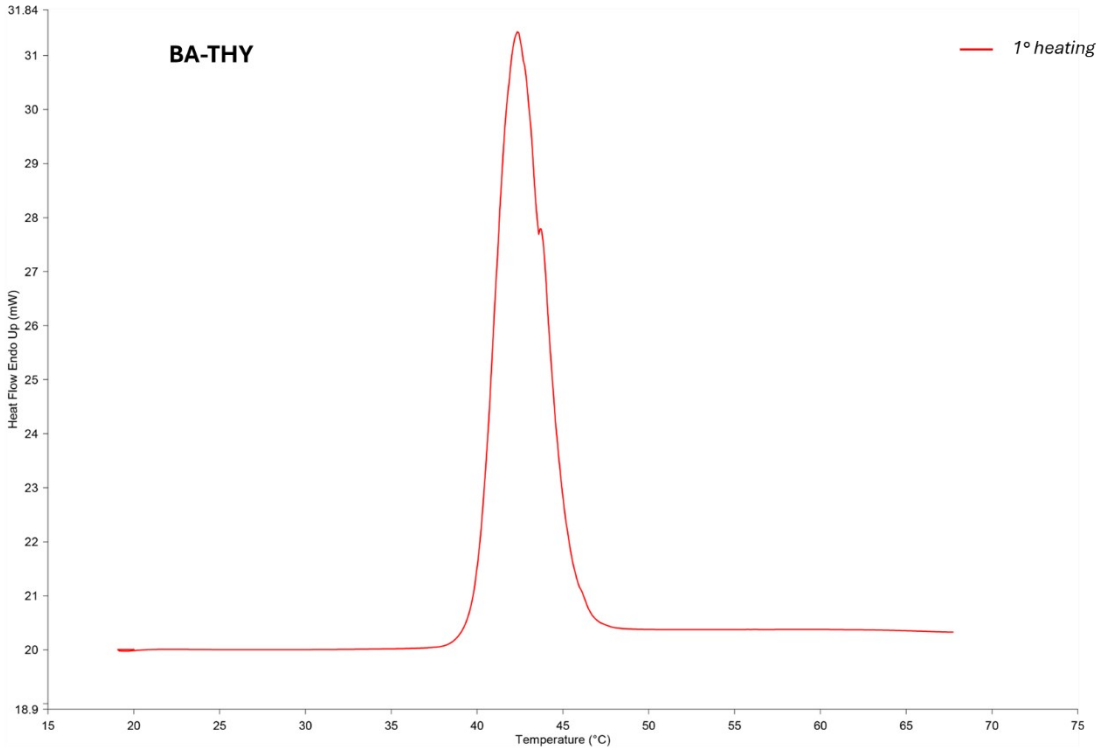

Figure S28. Thermogram of mixture BA-THY (χ_m(BA) = 0.3). Single heating run from 20 °C to 70 °C. The whole firing profile was performed at 5°C/min. The endothermic peak refers to the melting of the eutectic mixture between BA and THY.

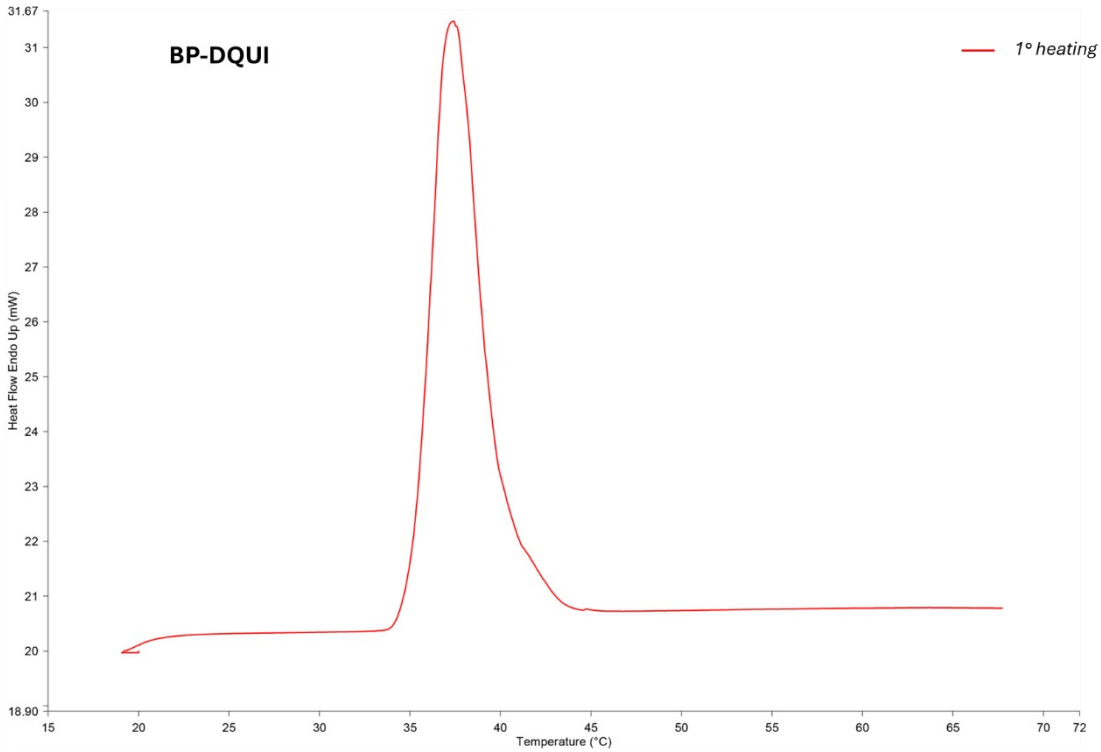

Figure S29. Thermogram of mixture BP-DQUI (χ_m(BP) = 0.7). Single heating run from 20 °C to 70 °C. The whole firing profile was performed at 5°C/min. The endothermic peak refers to the melting of the eutectic mixture between BP and DQUI.

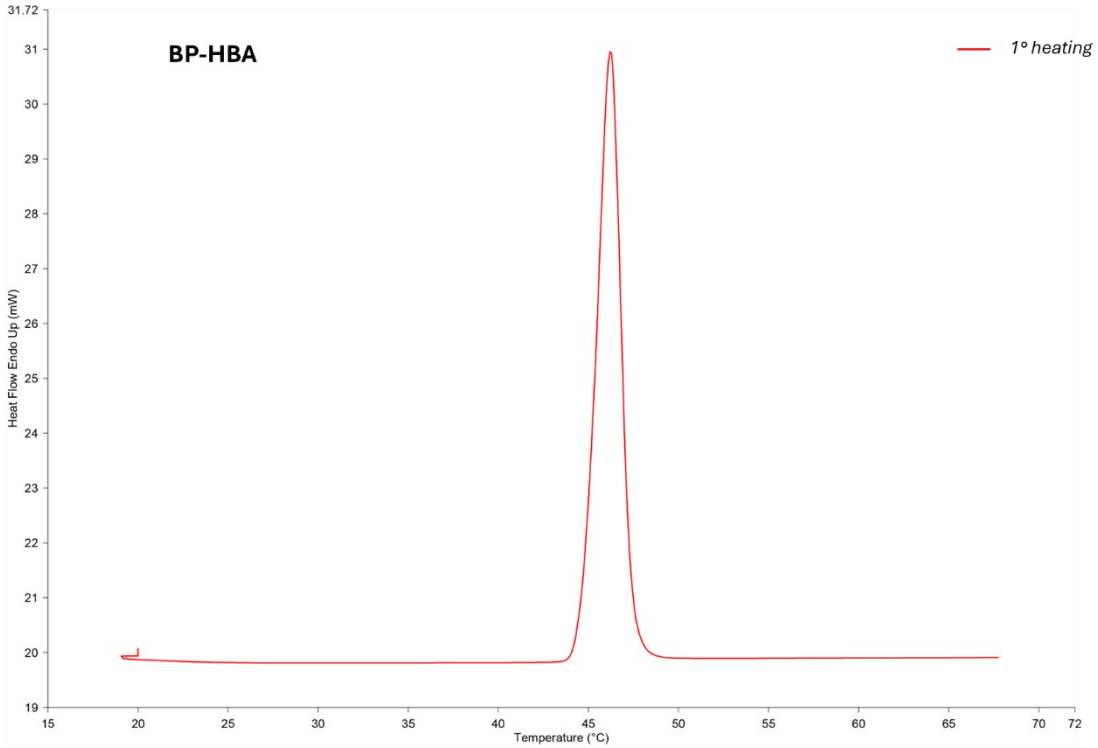

Figure S30. Thermogram of mixture BP-HBA (χ_m(BP) = 0.8). Single heating run from 20 °C to 70 °C. The whole firing profile was performed at 5°C/min. The endothermic peak refers to the melting of the eutectic mixture between BP and HBA.

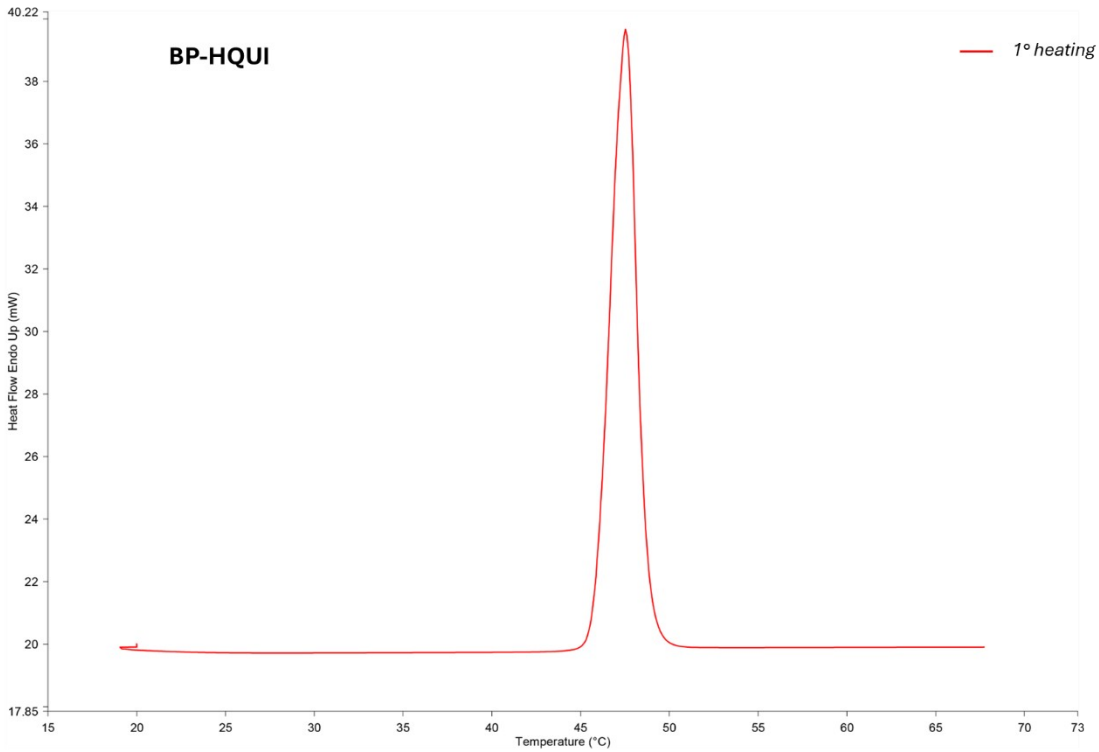

Figure S31. Thermogram of mixture BP-HQUI (χ_m(BP) = 0.8). Single heating run from 20 °C to 70 °C. The whole firing profile was performed at 5°C/min. The endothermic peak refers to the melting of the eutectic mixture between BP and HQUI.

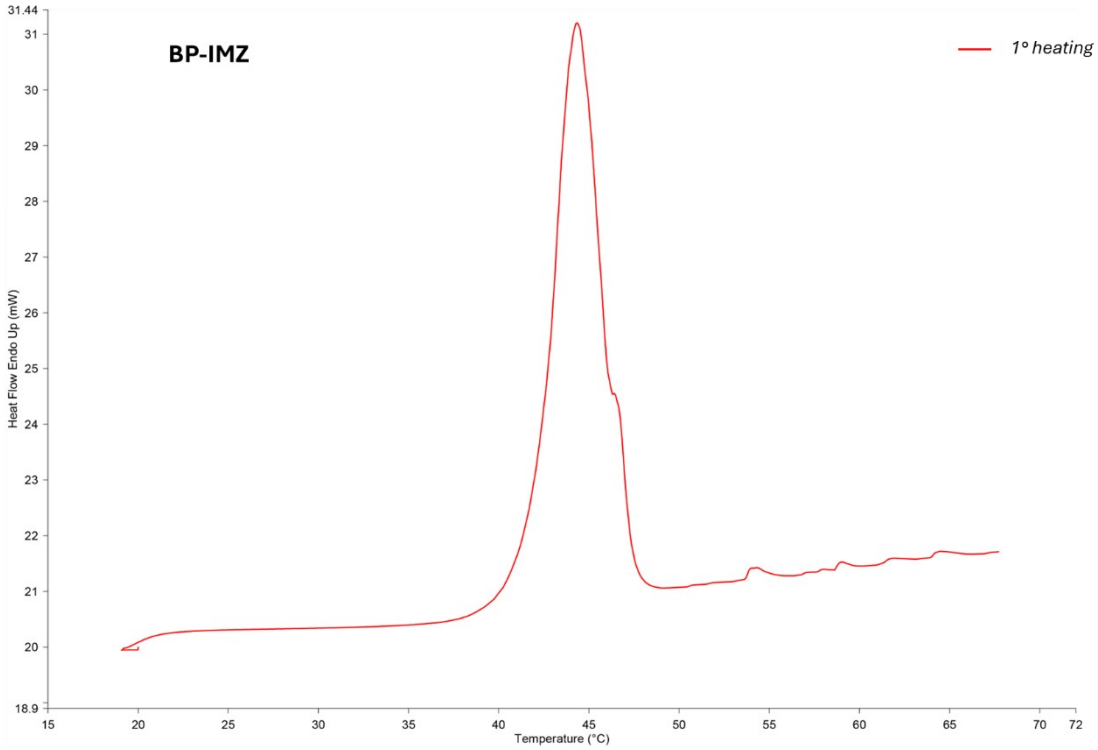

Figure S32. Thermogram of mixture BP-IMZ (χ_m(BP) = 0.6). Single heating run from 20 °C to 70 °C. The whole firing profile was performed at 5°C/min. The endothermic peak refers to the melting of the eutectic mixture between BP and IMZ.

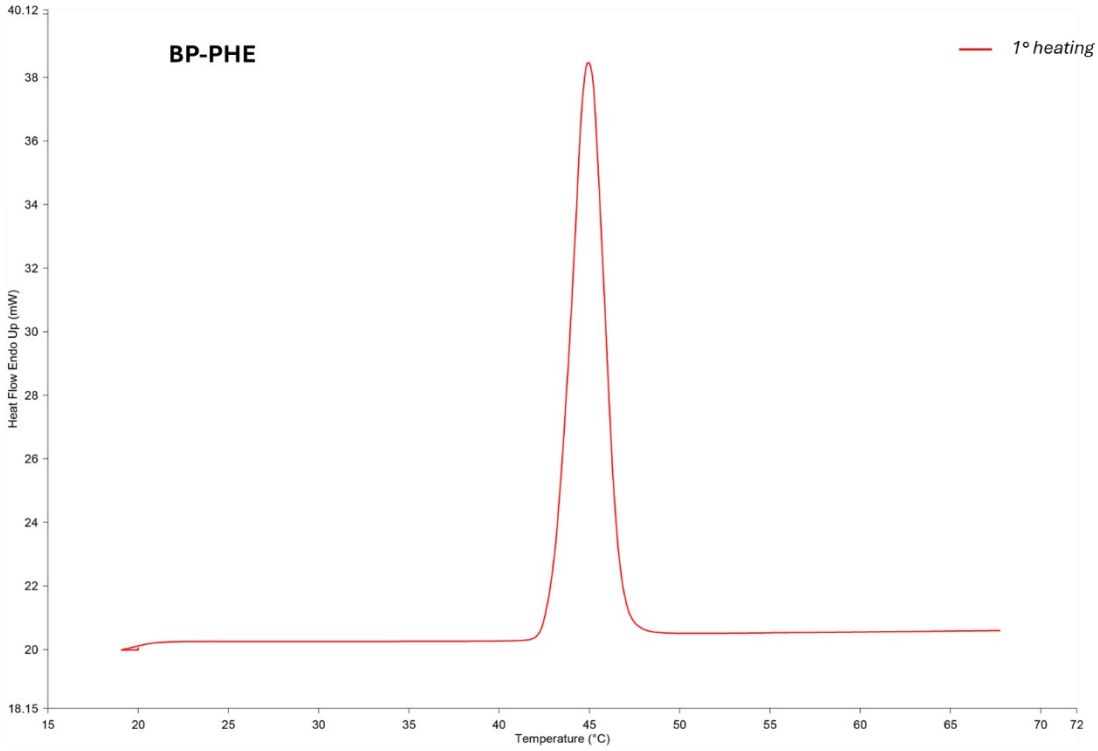

Figure S33. Thermogram of mixture BP-PHE (χ_m(BP) = 0.8). Single heating run from 20 °C to 70 °C. The whole firing profile was performed at 5°C/min. The endothermic peak refers to the melting of the eutectic mixture between BP and PHE.

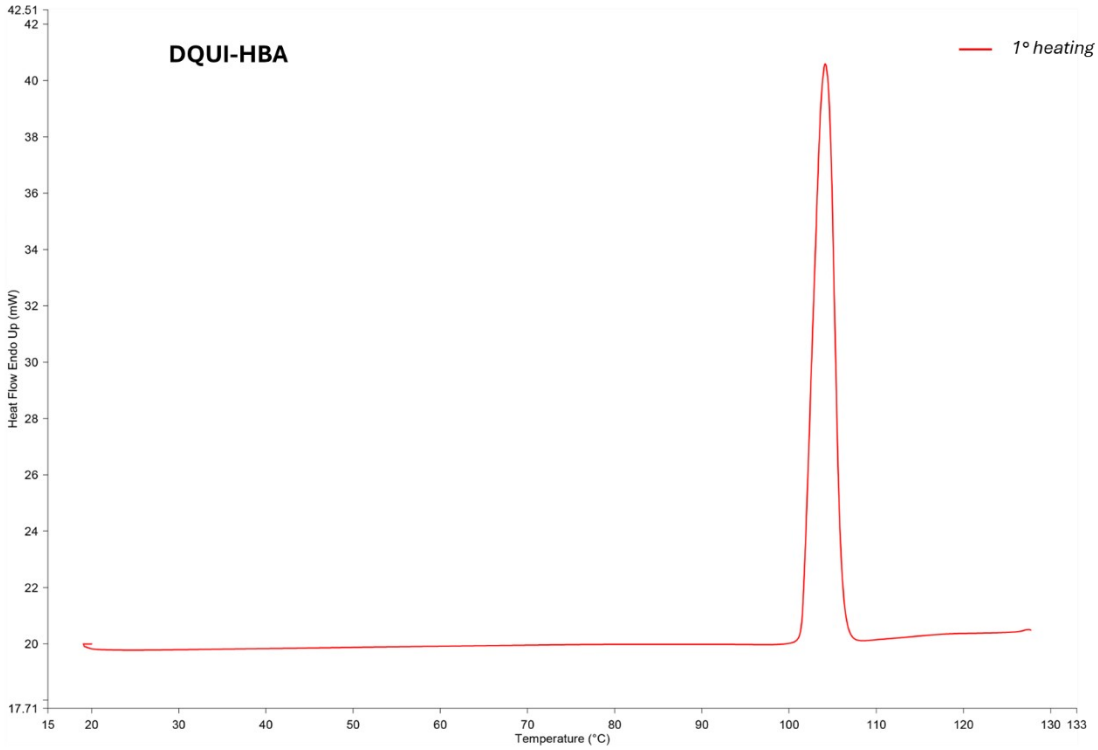

Figure S34. Thermogram of mixture DQUI-HBA (χ_m(DQUI) = 0.8). Single heating run from 20 °C to 130 °C. The whole firing profile was performed at 5°C/min. The endothermic peak refers to the melting of the eutectic mixture between DQUI and HBA.

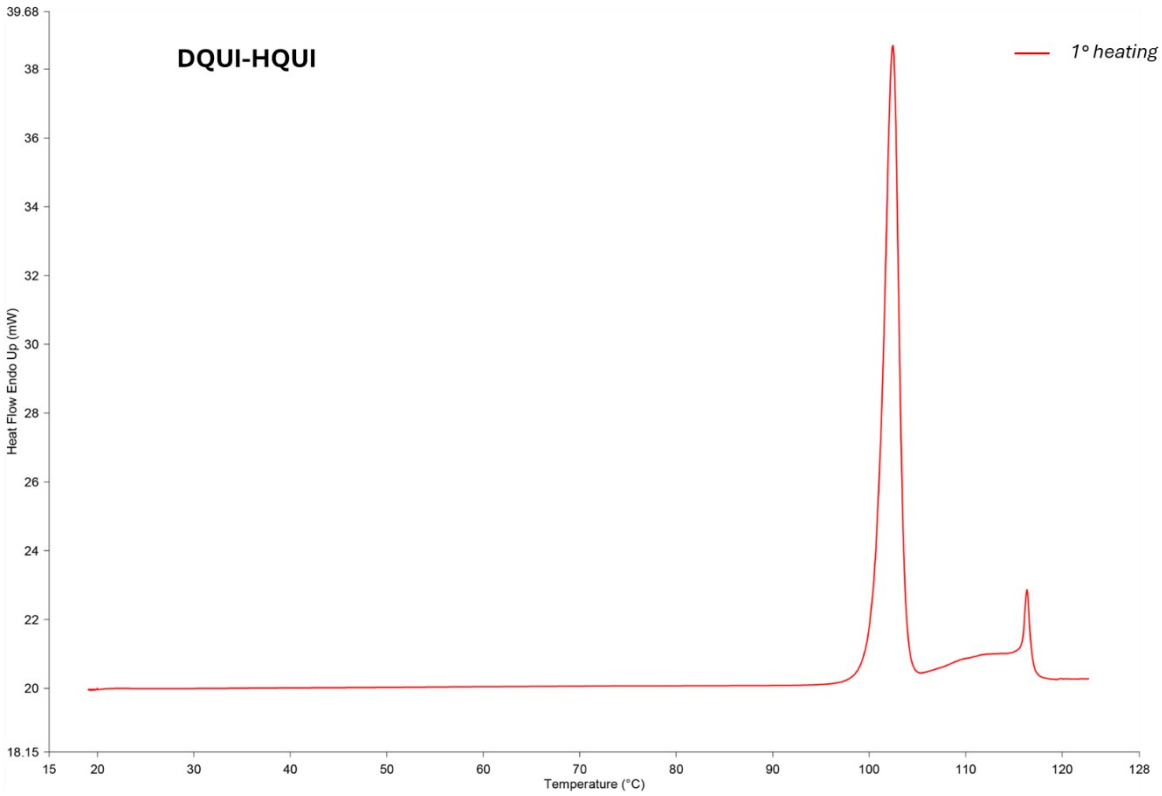

Figure S35. Thermogram of mixture DQUI-HQUI (χ_m(DQUI) = 0.8). Single heating run from 20 °C to 125 °C. The whole firing profile was performed at 5°C/min. The endothermic peak at 102.46 °C refers to the melting of the eutectic mixture between DQUI and HQUI, followed by the melting of residual HQUI at 116.35 °C.

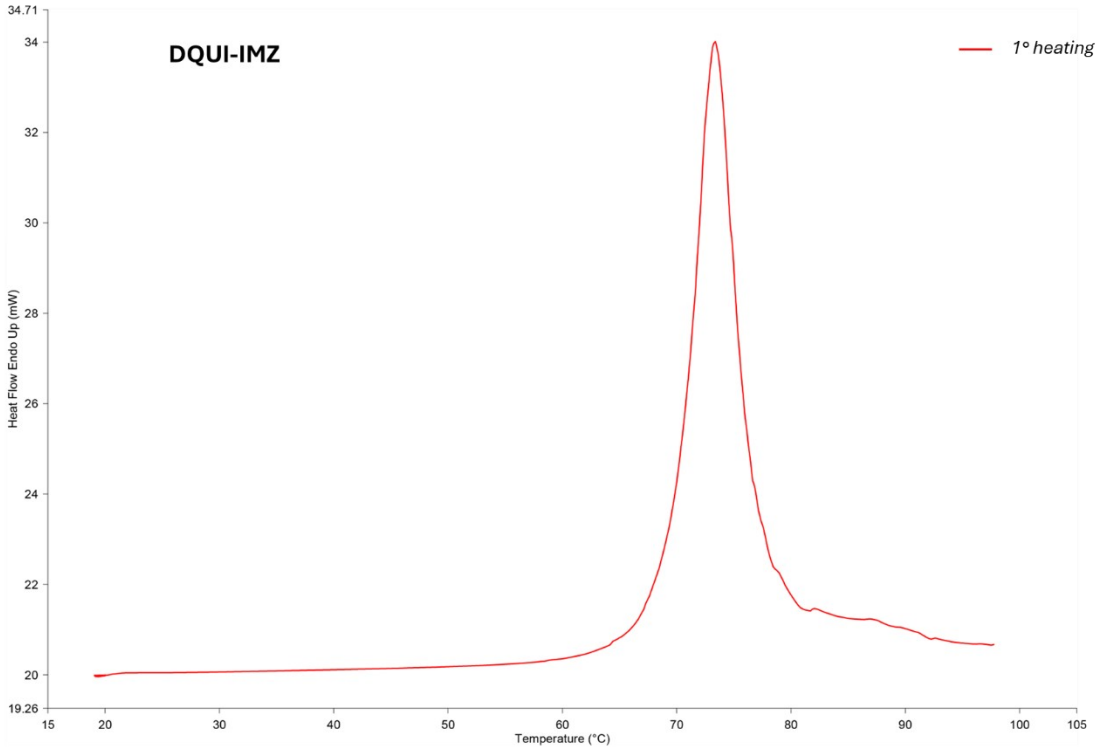

Figure S36. Thermogram of mixture DQUI-IMZ (χ_m(DQUI) = 0.3). Single heating run from 20 °C to 100 °C. The whole firing profile was performed at 5°C/min. The endothermic peak at 73.38 °C refers to the melting of the eutectic mixture between DQUI and IMZ, followed by the melting of residual HQUI at 87.46 °C.

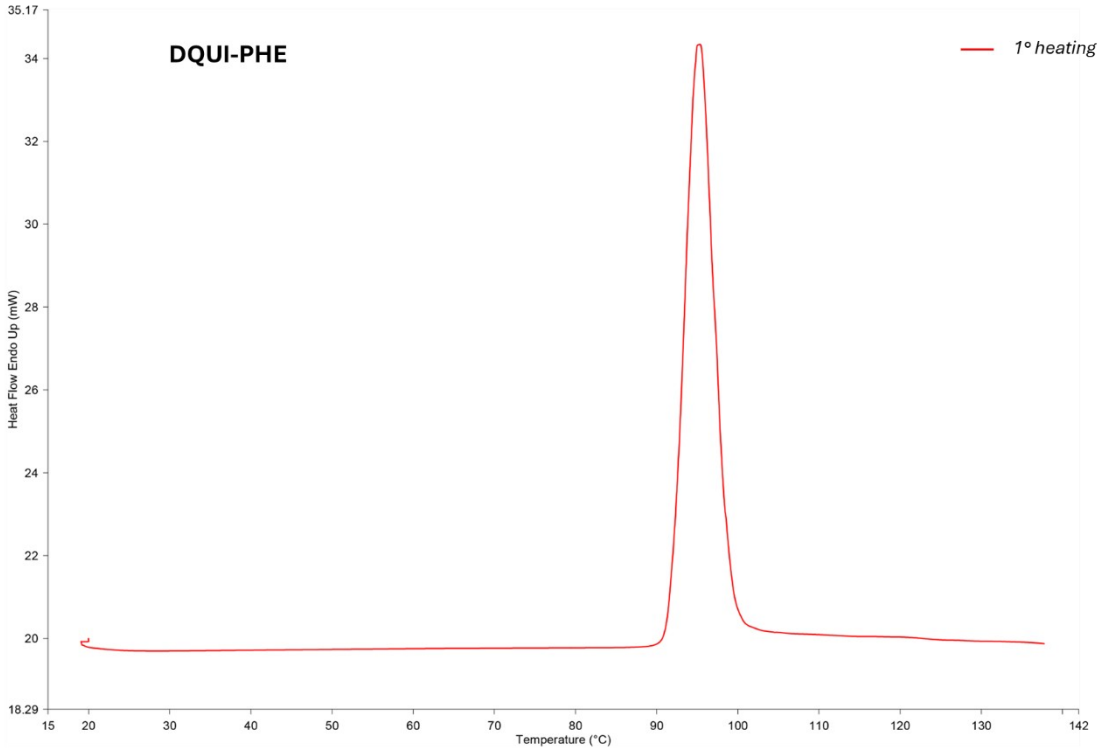

Figure S37. Thermogram of mixture DQUI-PHE (χ_m(DQUI) = 0.8). Single heating run from 20 °C to 140 °C. The whole firing profile was performed at 5°C/min. The endothermic peak refers to the melting of the eutectic mixture between DQUI and PHE.

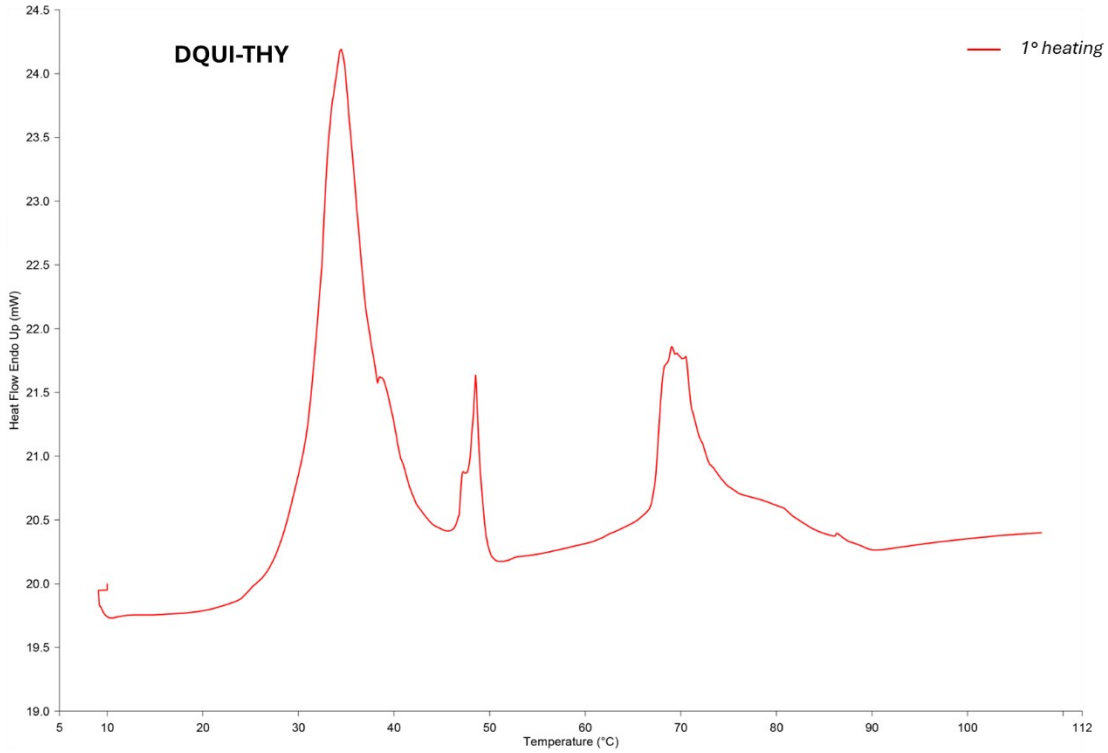

Figure S38. Thermogram of mixture DQUI-THY (χ_m(DQUI) = 0.3). Single heating run from 20 °C to 110 °C. The whole firing profile was performed at 5°C/min. The endothermic peak at 34.41 °C refers to the melting of the eutectic mixture between DQUI and THY. The following thermal event are of difficult interpretation but included the melting of residual THY.

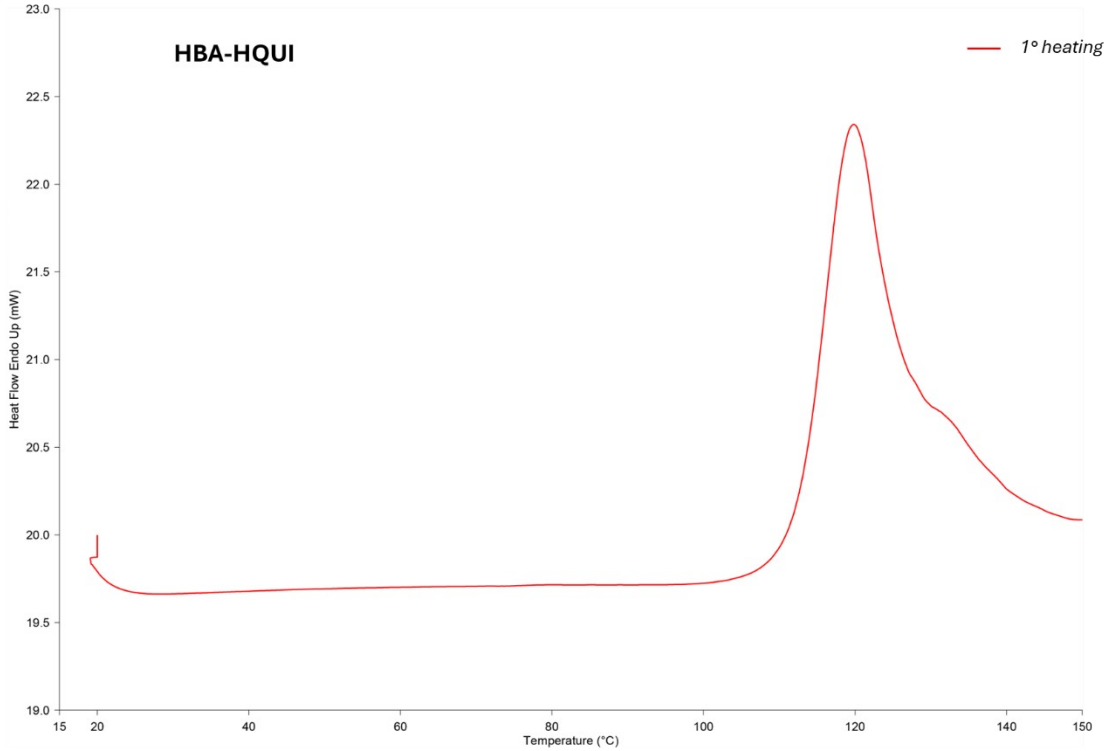

Figure S39. Thermogram of mixture HBA-HQUI (χ_m(HBA) = 0.4). Single heating run from 20 °C to 150 °C. The whole firing profile was performed at 5°C/min. The endothermic peak refers to the melting of the eutectic mixture between HBA and HQUI.

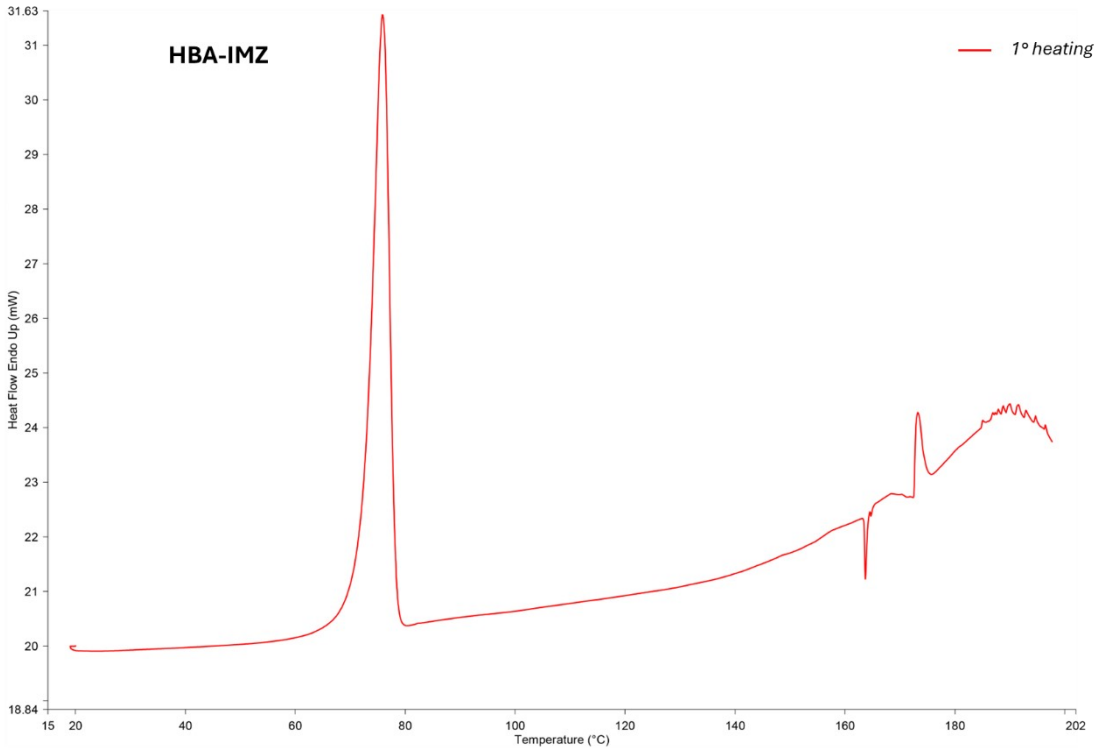

Figure S40. Thermogram of mixture HBA-IMZ (χ_m(HBA) = 0.2). Single heating run from 20 °C to 200 °C. The whole firing profile was performed at 5°C/min. The endothermic peak at 75.85 °C refers to the melting of the eutectic mixture between HBA and IMZ. The following thermal events are of difficult interpretation but included the melting of residual HBA.

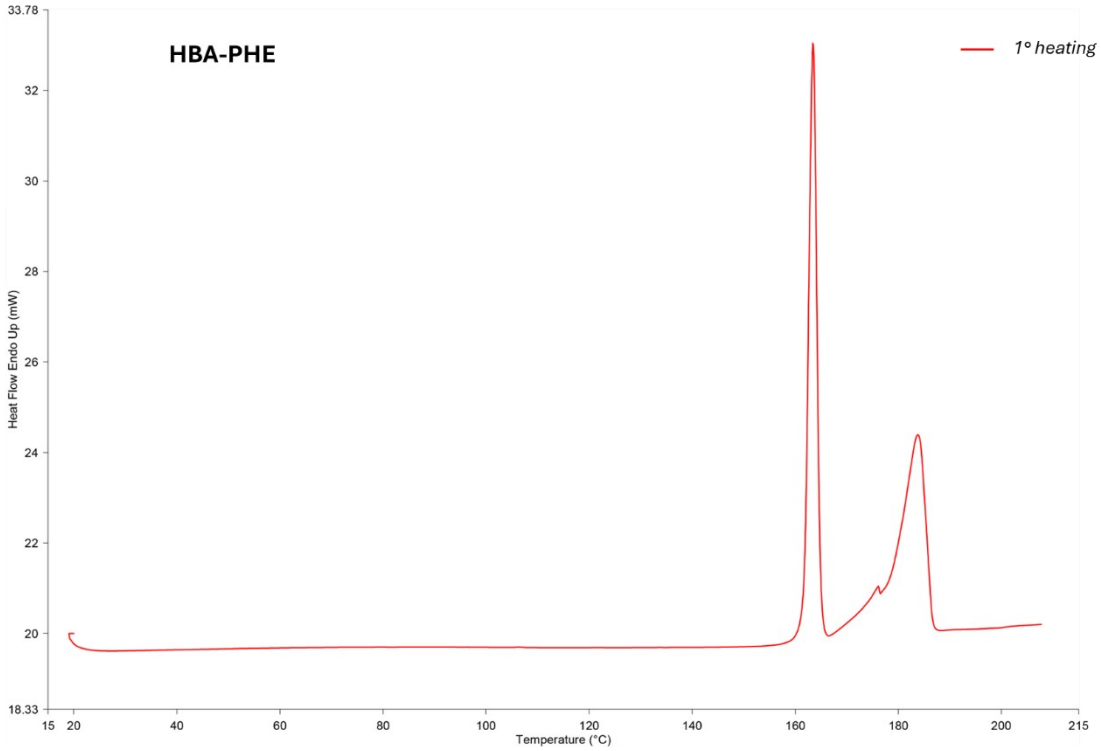

Figure S41. Thermogram of mixture HBA-PHE (χ_m(HBA) = 0.3). Single heating run from 20 °C to 210 °C. The whole firing profile was performed at 5°C/min. The endothermic peak at 163.40 °C refers to the melting of the eutectic mixture between HBA and PHE, followed by the melting of residual HBA at 183.82 °C.

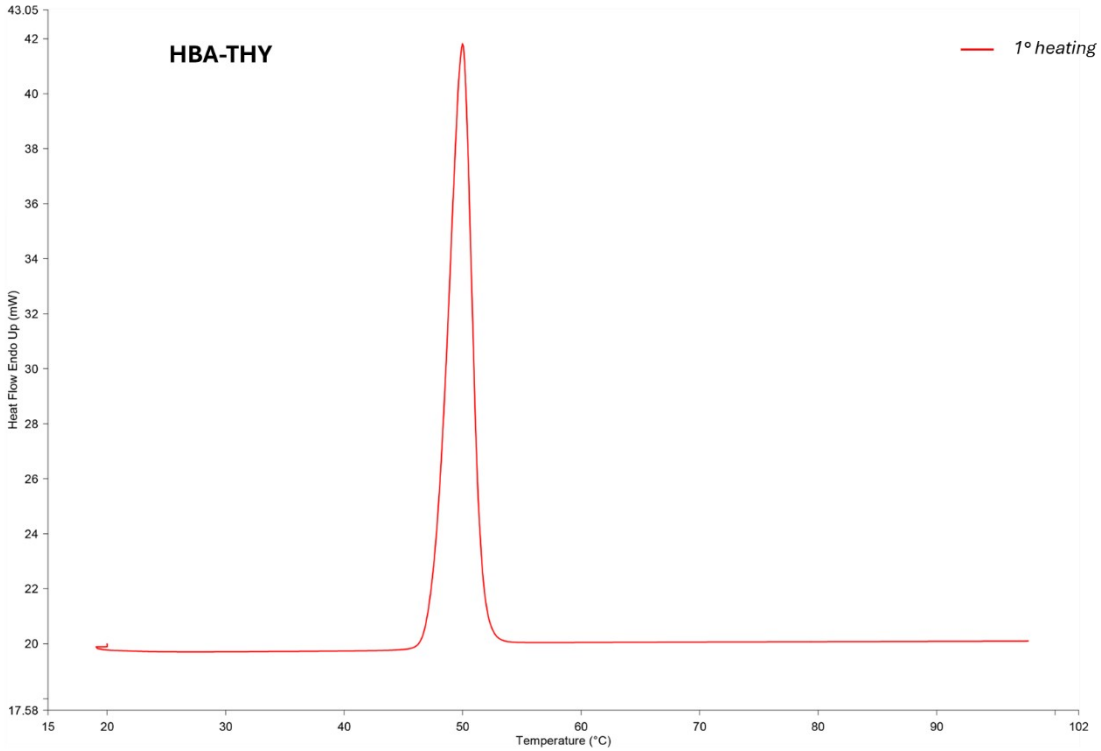

Figure S42. Thermogram of mixture HBA-THY (χ_m(HBA) = 0.2). Single heating run from 20 °C to 100 °C. The whole firing profile was performed at 5°C/min. The endothermic peak refers to the melting of the eutectic mixture between HBA and THY.

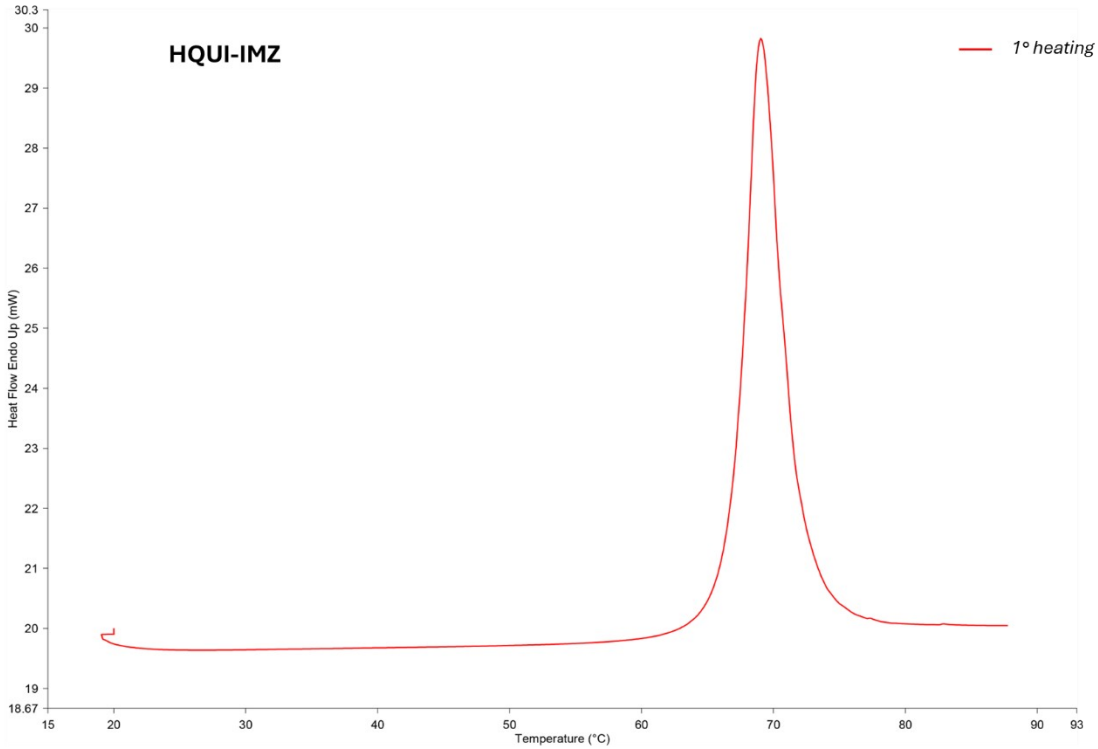

Figure S43. Thermogram of mixture HQUI-IMZ (χ_m(HQUI) = 0.2). Single heating run from 20 °C to 90 °C. The whole firing profile was performed at 5°C/min. The endothermic peak refers to the melting of the eutectic mixture between HQUI and IMZ.

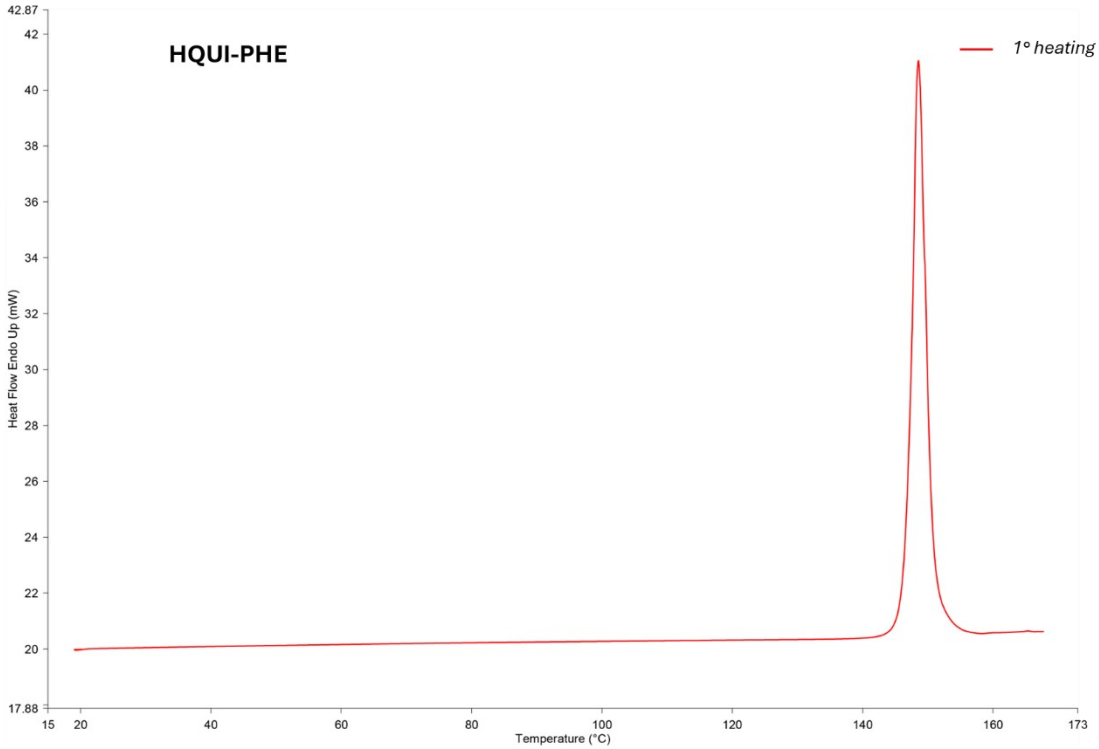

Figure S44. Thermogram of mixture HQUI-PHE (χ_m(HQUI) = 0.4). Single heating run from 20 °C to 170 °C. The whole firing profile was performed at 5°C/min. The endothermic peak refers to the melting of the eutectic mixture between HQUI and PHE.

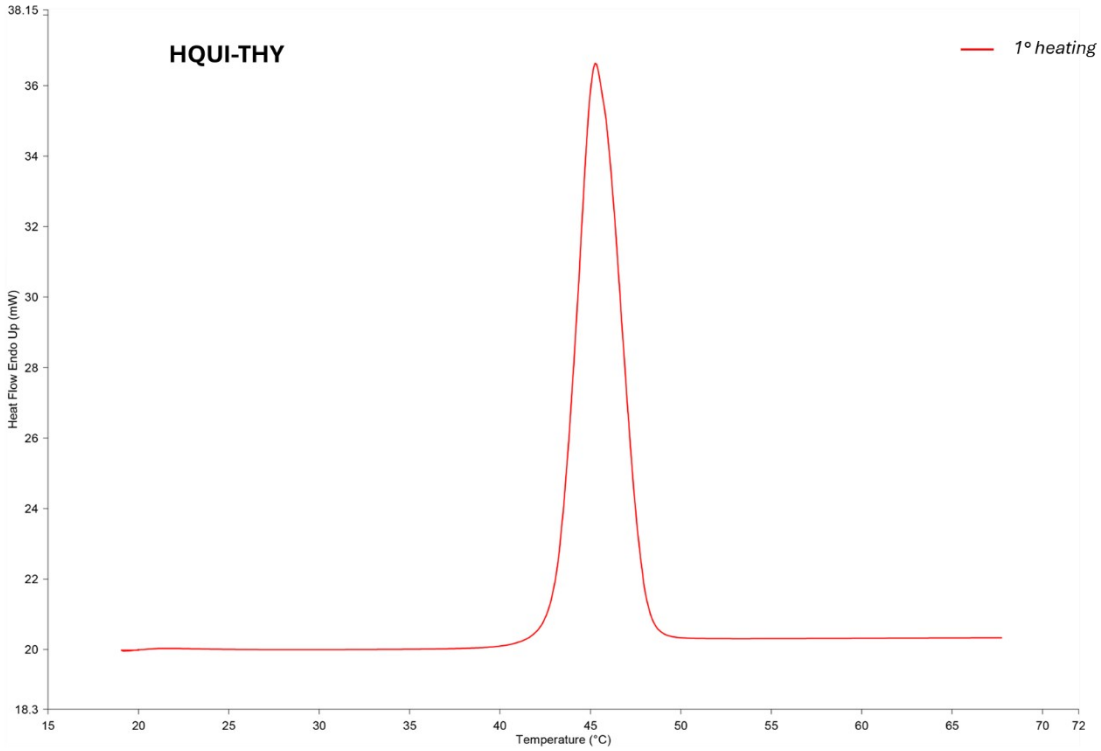

Figure S45. Thermogram of mixture HQUI-THY (χ_m(HQUI) = 0.2). Single heating run from 20 °C to 70 °C. The whole firing profile was performed at 5°C/min. The endothermic peak refers to the melting of the eutectic mixture between HQUI and THY.

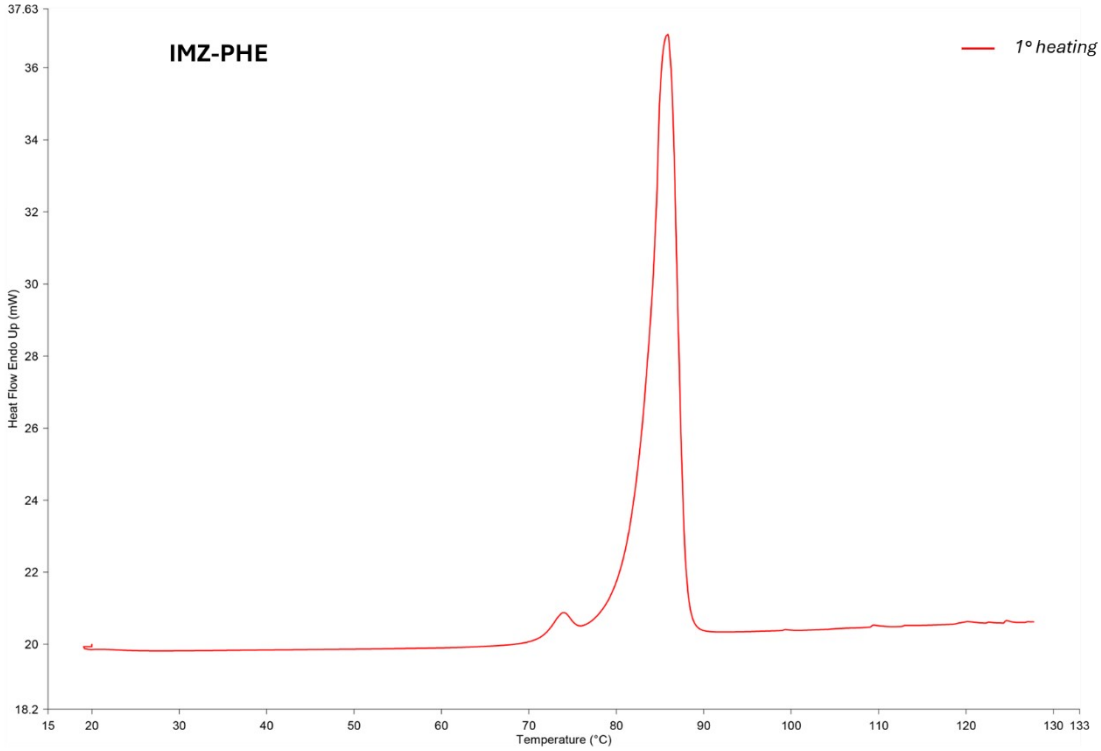

Figure S46. Thermogram of mixture IMZ-PHE (χ_m(IMZ) = 0.8). Single heating run from 20 °C to 130 °C. The whole firing profile was performed at 5°C/min. The endothermic peak refers to the melting of the eutectic mixture between IMZ and PHE, which occurred in concomitance of an exothermic event of difficult interpretation.

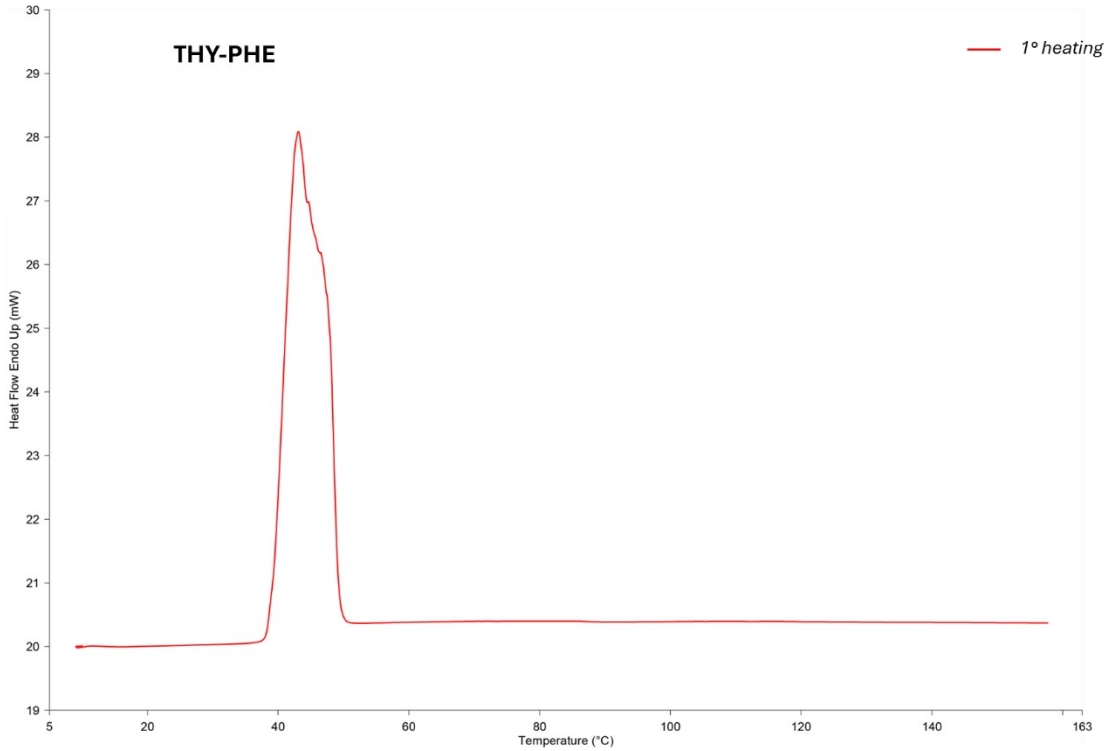

Figure S47. Thermogram of mixture PHE-THY (χ_m(PHE) = 0.2). Single heating run from 20 °C to 160 °C. The whole firing profile was performed at 5°C/min. The endothermic peak refers to the melting of the eutectic mixture between PHE and THY.

Table S2. Summary of the thermal events that occurred during DSC measurements of binary mixtures.

Binary mixture	*Run*		*Thermal event*	*Temperature (°C)*	*ΔH (J g⁻¹)*
APY-BA *(χ_m(APY) = 0.3)*	First heating	1st peak	Endothermic	44.64	3.64
		2nd peak	Endothermic	55.07	1.19
			Endothermic	75.86	34.85
		multiple peaks	Exothermic	85.76	-6.76
			Endothermic	93.88	9.34
APY-BP *(χ_m(APY) = 0.2)*	First heating	1st peak	Endothermic	46.45	91.51
APY-DQUI *(χ_m(APY) = 0.2)*	First heating	1st peak	Endothermic	104.83	109.73
		2nd peak	Endothermic	130.69	48.83
APY-HBA *(χ_m(APY) = 0.7)*	First heating	1st peak	Endothermic	64.65	0.85
		2nd peak	Endothermic	84.98	1.10
		3rd peak	Endothermic	124.55	106.03
		4th peak	Endothermic	169.07	194.72
APY-HQUI *(χ_m(APY) = 0.7)*	First heating	1st peak	Endothermic	105.52	126.15
		2nd peak	Endothermic	120.38	44.16
APY-IMZ *(χ_m(APY) = 0.3)*	First heating	1st peak	Endothermic	70.01	150.56
APY-PHE *(χ_m(APY) = 0.6)*	First heating	1st peak	Endothermic	100.55	0.58
		2nd peak	Endothermic	144.77	190.16
BA-BP *(χ_m(BA) = 0.3)*	First heating	1st peak	Endothermic	41.90	99.01
BA-DQUI *(χ_m(BA) = 0.4)*	First heating	1st peak	Endothermic	46.85	56.04
		2nd peak	Endothermic	83.56	65.54
BA-HBA *(χ_m(BA) = 0.8)*	First heating	1st peak	Endothermic	114.20	141.60
BA-HQUI *(χ_m(BA) = 0.8)*	First heating	1st peak	Endothermic	83.49	45.27
		2nd peak	Endothermic	112.20	74.02
BA-IMZ *(χ_m(BA) = 0.3)*	First heating	1st peak	Endothermic	53.12	74.40
		2nd peak	Exothermic	63.30	-8.03
BA-PHE *(χ_m(BA) = 0.7)*	First heating	1st peak	Endothermic	87.94	80.32
BA-THY *(χ_m(BA) = 0.3)*	First heating	1st peak	Endothermic	42.35	122.27
BP-DQUI *(χ_m(BP) = 0.7)*	First heating	1st peak	Endothermic	37.43	105.98
BP-HBA *(χ_m(BP) = 0.8)*	First heating	1st peak	Endothermic	46.19	89.75
BP-HQUI *(χ_m(BP) = 0.8)*	First heating	1st peak	Endothermic	47.52	89.67
BP-IMZ *(χ_m(BP) = 0.6)*	First heating	1st peak	Endothermic	44.36	78.08
BP-PHE *(χ_m(BP) = 0.8)*	First heating	1st peak	Endothermic	44.97	88.59
DQUI-HBA *(χ_m(DQUI) = 0.8)*	First heating	1st peak	Endothermic	114.18	118.91
DQUI-HQUI *(χ_m(DQUI) = 0.8)*	First heating	1st peak	Endothermic	102.46	113.35
		2nd peak	Endothermic	116.35	30.84
DQUI-IMZ *(χ_m(DQUI) = 0.3)*	First heating	1st peak	Endothermic	73.38	112.89
		2nd peak	Endothermic	87.46	29.02
DQUI-PHE *(χ_m(DQUI) = 0.8)*	First heating	1st peak	Endothermic	95.38	112.70
DQUI-THY *(χ_m(DQUI) = 0.3)*	First heating	1st peak	Endothermic	34.41	41.04
		2nd peak	Endothermic	48.54	14.34
		3rd peak	Endothermic	69.04	24.61
HBA-HQUI *(χ_m(HBA) = 0.4)*	First heating	1st peak	Endothermic	120.52	63.60
HBA-IMZ *(χ_m(HBA) = 0.2)*	First heating	1st peak	Endothermic	75.85	85.14
		2nd peak	Exothermic	163.71	-1.19

		3rd peak	Endothermic	173.24	3.82
HBA-PHE	First heating	1st peak	Endothermic	163.40	57.42
(χ_m(HBA) = 0.3)		2nd peak	Endothermic	183.82	69.48

Table S2 ***Continued.*** Summary of the thermal events that occurred during DSC measurements of binary mixtures.

Binary mixture	***Run***		***Thermal event***	***Temperature (°C)***	***ΔH (J g^{-1})***
HBA-THY *(χ_m(HBA) = 0.2)*	First heating	1st peak	Endothermic	49.98	121.66
HQUI-IMZ *(χ_m(HQUI) = 0.2)*	First heating	1st peak	Endothermic	69.04	133.71
HQUI-PHE *(χ_m(HQUI) = 0.4)*	First heating	1st peak	Endothermic	148.58	141.91
HQUI-THY *(χ_m(HQUI) = 0.2)*	First heating	1st peak	Endothermic	45.25	118.36
IMZ-PHE	First heating	1st peak	Exothermic	76.72	-4.88
(χ_m(IMZ) = 0.8)		2nd peak	Endothermic	85.91	126.21
PHE-THY *(χ_m(PHE) = 0.2)*	First heating	1st peak	Endothermic	43.17	114.24

Interaction parameter (χ) calculations

The general Schroder-Laar equation (Eq. S1) defines the solid-liquid equilibrium curve of a component within a binary mixture, also accounting for non-ideality by including parameter χ from Regular Solutions' theory[1]:

$$\ln\ (x_i) + \chi\ (1 - x_i)^2 = \frac{\Delta H_i}{R}\left(\frac{1}{T_i} - \frac{1}{T_{calc}}\right) \qquad \textit{Eq. S1}$$

Given a generic binary mixture 1-2, the equilibrium curves of two components must assume the same value at the eutectic point (Eq. S2), where $T_{calc} = T_{eut}$. By imposing that the equilibrium curves intersect at T_{eut}, a single equation is returned (Eq. S3) wherein the only unknown quantities are the molar ratio at the eutectic composition x_{eut} and the interaction parameter χ.

$$\frac{1}{T_{eut}} = \frac{1}{T_1} - \frac{R}{\Delta H_1}\left[ln\ x_1 + \chi\ (1 - x_1)^2\right] = \frac{1}{T_2} - \frac{R}{\Delta H_2}\left[ln\ (1 - x_1) + \chi\ (x_1)^2\right] \qquad \textit{Eq. S2}$$

$$\frac{\left[ln\ x_{eut} + \chi\ (1 - x_{eut})^2\right]}{\Delta H_1} - \frac{\left[ln\ (1 - x_{eut}) + \chi\ (x_{eut})^2\right]}{\Delta H_2} - \frac{1}{RT_1} + \frac{1}{RT_2} = 0 \qquad \textit{Eq. S3}$$

The minimization of Eq S3 returns the two unknown quantities (x_{eut}, χ) and it is implemented into our predictive software PoEM (*i.e.* Predictor of Eutectic Mixtures) as SciPy optimize function[2], used for both calculating the eutectic point of a non-ideal binary mixture or the tables of potential molecular partners suitable for a defined molecule of interest. Once determined x_{eut} and χ, the melting temperature of eutectic mixtures were calculated according to Eq. S1.

The calculation of the interaction parameter χ for the training set of binary mixtures was performed using the experimental melting temperature of eutectic mixtures (T_{eut}) determined through DSC measurements. After substituting T_{eut} into the solid-liquid equilibrium curves of two components (Eq. S2), the resulting expressions were imposed to return the same values by varying x_{eut} and χ. The melting temperatures and enthalpies of pure components used in the calculations were experimentally determined through DSC analysis (see Table S1). Table S3 resumes the experimental (T_1, ΔH_1, T_2, ΔH_2, T_{eut}) and calculated (X_{eut}, χ) parameters for the training set of binary mixtures.

Table S3. Summary of parameters used for calculating the eutectic composition X_{eut} and the interaction parameter χ for the training set of binary mixtures.

Binary mixture 1-2	T_1 **(K)**	ΔH_1 **(kJ mol⁻¹)**	T_2 **(K)**	ΔH_2 **(kJ mol⁻¹)**	X_{eut}	T_{eut} **(K)**	χ
APY-BA *(x_m(APY) = 0.3)*	431.52	19.75	396.20	17.27	0.44	317.79	-3.68
APY-BP *(x_m(APY) = 0.2)*	431.52	19.75	321.04	20.25	0.03	319.60	1.51
APY-DQUI *(x_m(APY) = 0.2)*	431.52	19.75	379.26	21.33	0.02	377.98	3.08
APY-HBA *(x_m(APY) = 0.7)*	431.52	19.75	488.20	35.38	0.71	397.70	-1.49
APY-HQUI *(x_m(APY) = 0.7)*	431.52	19.75	468.04	24.78	0.60	378.67	-1.63
APY-IMZ *(x_m(APY) = 0.3)*	431.52	19.75	363.24	12.79	0.22	343.16	0.14
APY-PHE *(x_m(APY) = 0.6)*	431.52	19.75	447.13	24.24	0.76	417.92	1.67

APY-THY* (χ_m*(APY) = 0.2)*	431.52	19.75	323.48	17.96	0.32	293.15	-3.11
BA-BP (χ_m*(BA) = 0.3)*	396.20	17.27	321.04	20.25	0.15	315.05	0.76

Table S3 Continued. Summary of parameters used for calculating the eutectic composition X_{eut} and the interaction parameter χ for the training set of binary mixtures.

Binary mixture 1-2	T_1 **(K)**	ΔH_1 ***(kJ mol⁻¹)***	T_2 **(K)**	ΔH_2 ***(kJ mol⁻¹)***	X_{eut}	T_{eut} **(K)**	χ
BA-DQUI (χ_m*(BA) = 0.4)*	396.20	17.27	379.26	21.33	0.50	320.00	-2.24
BA-HBA (χ_m*(BA) = 0.8)*	396.20	17.27	488.20	35.38	0.88	387.35	-0.11
BA-HQUI (χ_m*(BA) = 0.8)*	396.20	17.27	468.04	24.78	0.68	356.64	-1.87
BA-IMZ (χ_m*(BA) = 0.3)*	396.20	17.27	363.24	12.79	0.36	326.27	-0.24
BA-PHE (χ_m*(BA) = 0.7)*	396.20	17.27	447.13	24.24	0.67	361.09	-1.00
BA-THY (χ_m*(BA) = 0.3)*	396.20	17.27	323.48	17.96	0.17	315.50	0.62
BP-DQUI (χ_m*(BP) = 0.7)*	321.04	20.25	379.26	21.33	0.77	310.58	-0.01
BP-HBA (χ_m*(BP) = 0.8)*	321.04	20.25	488.20	35.38	0.96	319.34	-1.45
BP-HQUI (χ_m*(BP) = 0.8)*	321.04	20.25	468.04	24.78	0.99	320.67	1.83
BP-IMZ (χ_m*(BP) = 0.6)*	321.04	20.25	363.24	12.79	0.90	317.51	2.10
BP-PHE (χ_m*(BP) = 0.8)*	321.04	20.25	447.13	24.24	0.93	318.12	0.05
BP-THY* (χ_m*(BP) = 0.4)*	321.04	20.25	323.48	17.96	0.49	293.15	-0.07
DQUI-HBA (χ_m*(DQUI) = 0.8)*	379.26	21.33	488.20	35.38	0.98	387.33	0.84
DQUI-HQUI (χ_m*(DQUI) = 0.8)*	379.26	21.33	468.04	24.78	0.93	375.61	1.27
DQUI-IMZ (χ_m*(DQUI) = 0.3)*	379.26	21.33	363.24	12.79	0.25	346.53	1.33
DQUI-PHE (χ_m*(DQUI) = 0.8)*	379.26	21.33	447.13	24.24	0.81	368.53	0.40
DQUI-THY (χ_m*(DQUI) = 0.3)*	379.26	21.33	323.48	17.96	0.27	307.56	-0.49
HBA-HQUI (χ_m*(HBA) = 0.4)*	488.20	35.38	468.04	24.78	0.38	393.67	-3.69
HBA-IMZ (χ_m*(HBA) = 0.2)*	488.20	35.38	363.24	12.79	0.13	349.00	-1.90
HBA-PHE (χ_m*(HBA) = 0.3)*	488.20	35.38	447.13	24.24	0.17	436.55	1.06
HBA-THY (χ_m*(HBA) = 0.2)*	488.20	35.38	323.48	17.96	0.01	323.13	0.47
HQUI-IMZ (χ_m*(HQUI) = 0.2)*	468.04	24.78	363.24	12.79	0.19	342.19	-1.09
HQUI-PHE (χ_m*(HQUI) = 0.4)*	468.04	24.78	447.13	24.24	0.39	421.73	0.65
HQUI-THY (χ_m*(HQUI) = 0.2)*	468.04	24.78	323.48	17.96	0.09	318.40	-0.78
IMZ-PHE (χ_m*(IMZ) = 0.8)*	363.24	12.79	447.13	24.24	0.05	359.06	1.52
IMZ-THY* (χ_m*(IMZ) = 0.4)*	363.24	12.79	323.48	17.96	0.36	293.15	-0.57
PHE-THY (χ_m*(PHE) = 0.2)*	447.13	24.24	323.48	17.96	0.13	316.32	-0.85

*Binary mixtures which melt at laboratory conditions (293.15 K, 1 atm).

Interaction energy ($\Delta\Delta G$) calculations

Interaction energies were calculated starting from the molecular electrostatic potential (MEP) surface for all components of binary mixtures. Calculations of MEP surfaces were performed by Crystal Explorer17 on crystal structures reported in Table S4, which are available at CSD.

Table S4. Crystal structures of components used for MEP surface calculations with corresponding CSD Refcodes.

Component	*CSD Refcode*
APY	AMPYRE01
BA	BENZAC01
BP	BPHENO17
DQUI	KEYNOR
HBA	JOZZIH01
HQUI	QOVRUP
IMZ	IMAZOL04
PHE	PHENAZ04
THY	IPMEPL

MEP surfaces were generated at 6-31G(d) level of theory using either 0.0300 or 0.0104 e bohr^{-3} isodensity surfaces. These isodensity values have been recently optimised by Storer *et al.*[3] to account for secondary ionic interactions, the former (0.0300 e bohr^{-3}) used for estimating the maxima of MEP surfaces (E_{max}) while the latter (0.0104 e bohr^{-3}) for estimating the minima (E_{min}). After generating MEP surfaces, a pair of E_{max} and E_{min} values was extracted for each component and used for determining α and β parameters, according to Eq. S4-S5:

$$\alpha = m_{\alpha}E_{max} + c_{\alpha} \qquad \textit{Eq. S4}$$

$$\beta = m_{\beta}E_{min} + c_{\beta} \qquad \textit{Eq. S5}$$

m_{α}, m_{β}, c_{α}, c_{β} values were experimentally determined by Storer *et al.*[3,4] and depend on the functional groups associated with E_{max} and E_{min} values. A table of all parameters used for α and β calculations is here reported (Table S5).

Table S5. .List of parameters used for computing α *and* β *values for all components of binary mixtures.*

Component	E_{max} *(kJ mol^{-1})*	E_{min} *(kJ mol^{-1})*	m_{α}, c_{α}	m_{β}, c_{β}	α	β
APY	421.39	-294.84	0.0132, -2.8	-0.0336, -1.08	2.76	8.83
BA	549.52	-194.55	0.0132, -2.8	-0.0336, -0.42	4.45	6.12
BP	219.75	-194.02	0.0072, -0.17	-0.0336, -0.42	1.41	6.10
DQUI	211.62	-225.79	0.0072, -0.17	-0.0336, -1.08	1.35	6.51
HBA	534.29	-220.02	0.0132, -2.8	-0.0336, -0.42	4.25	6.97
HQUI	515.91	-257.04	0.0132, -2.8	-0.0336, -1.08	4.01	7.56
IMZ	471.28	-293.79	0.0132, -2.8	-0.0336, -1.08	3.42	8.79
PHE	234.46	-216.60	0.0072, -0.17	-0.0336, -1.08	1.52	6.20
THY	478.37	-138.89	0.0132, -2.8	-0.0336, -0.66	3.51	4.01

Considering intermolecular interactions as the product of the most polar functional groups belonging to different molecules (-$\alpha\,\beta$)[5], interaction energies ($\Delta\Delta G$) were obtained subtracting homomeric from heteromeric contributions, as defined by Eq. S6:

$$\Delta\Delta G/kJ\,mol^{-1} = \underbrace{(\alpha_1\beta_1 + \alpha_2\beta_2)}_{homomeric\ contribution} - \underbrace{(\alpha_1\beta_2 + \alpha_2\beta_1)}_{heteromeric\ contribution} \qquad \textit{Eq. S6}$$

Calculated interaction energies and χ values for the training set of binary mixtures are reported in Table S6.

Table S6. Interaction energies $\Delta\Delta G$ and interaction parameters χ calculated for the training set of binary mixtures.

Binary mixture	$\Delta\Delta G$ ***(kJ mol⁻¹)***	χ
APY-BA *(x_m(APY) = 0.3)*	-4.58	-3.68
APY-BP *(x_m(APY) = 0.2)*	3.68	1.51
APY-DQUI *(x_m(APY) = 0.2)*	3.27	3.08
APY-HBA *(x_m(APY) = 0.7)*	-2.76	-1.49
APY-HQUI *(x_m(APY) = 0.7)*	-1.58	-1.63
APY-IMZ *(x_m(APY) = 0.3)*	-0.02	0.14
APY-PHE *(x_m(APY) = 0.6)*	3.27	1.67
APY-THY *(x_m(APY) = 0.2)*	-3.62	-3.11
BA-BP *(x_m(BA) = 0.3)*	0.05	0.76
BA-DQUI *(x_m(BA) = 0.4)*	-1.21	-2.24
BA-HBA *(x_m(BA) = 0.8)*	-0.17	-0.11
BA-HQUI *(x_m(BA) = 0.8)*	-0.64	-1.87
BA-IMZ *(x_m(BA) = 0.3)*	-2.76	-0.24
BA-PHE *(x_m(BA) = 0.7)*	-0.24	-1.00
BA-THY *(x_m(BA) = 0.3)*	1.98	0.62
BP-DQUI *(x_m(BP) = 0.7)*	-0.02	-0.01
BP-HBA *(x_m(BP) = 0.8)*	2.48	-1.45
BP-HQUI *(x_m(BP) = 0.8)*	3.79	1.83
BP-IMZ *(x_m(BP) = 0.6)*	5.41	2.10
BP-PHE *(x_m(BP) = 0.8)*	0.01	0.05
BP-THY *(x_m(BP) = 0.4)*	-4.40	-0.07
DQUI-HBA *(x_m(DQUI) = 0.8)*	1.35	0.84
DQUI-HQUI	2.79	1.27

(χ_m(DQUI) = 0.8)		
DQUI-IMZ *(χ_m(DQUI) = 0.3)*	4.72	1.33
DQUI-PHE *(χ_m(DQUI) = 0.8)*	-0.05	0.40

Table S6 Continued. Interaction energies $\Delta\Delta G$ and interaction parameters χ calculated for the training set of binary mixtures.

DQUI-THY *(χ_m(DQUI) = 0.3)*	-5.40	-0.49
HBA-HQUI *(χ_m(HBA) = 0.4)*	-0.14	-3.69
HBA-IMZ *(χ_m(HBA) = 0.2)*	-1.51	-1.90
HBA-PHE *(χ_m(HBA) = 0.3)*	2.12	1.06
HBA-THY *(χ_m(HBA) = 0.2)*	2.19	0.47
HQUI-IMZ *(χ_m(HQUI) = 0.2)*	-0.73	-1.09
HQUI-PHE *(χ_m(HQUI) = 0.4)*	3.39	0.65
HQUI-THY *(χ_m(HQUI) = 0.2)*	1.76	-0.78
IMZ-PHE *(χ_m(IMZ) = 0.8)*	4.93	1.52
IMZ-THY *(χ_m(IMZ) = 0.4)*	-0.48	-0.57
PHE-THY *(χ_m(PHE) = 0.2)*	-4.37	-0.85

PoEM graphical interface

PoEM exhibits a simple graphical user interface (GUI) divided into two parts which differentiate for the type of calculations (*i.e. multi-tables* and *single-plot*) (Figure S48).

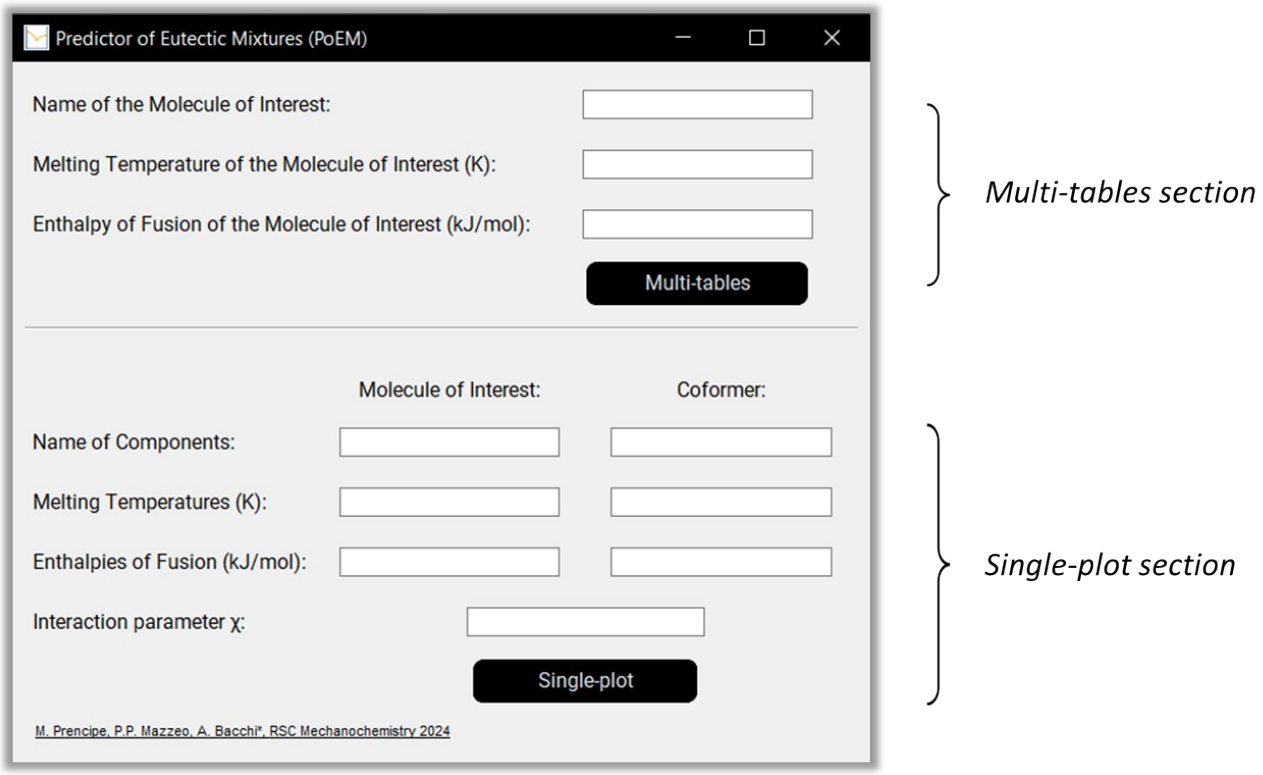

Figure S48. Graphical visualization of PoEM's GUI.

In the *multi-tables* section of PoEM's GUI, the tool calculates the eutectic point of binary mixtures obtained by combining a specific molecule of interest with 10x10 potential molecular partners. The input data are the enthalpy of fusion and the melting temperature of the molecule of interest. The output tables report X_{eut} and T_{eut} values for 10x10 simulated binary mixtures at 4 different χ values (-4, -2, 0 ,3), taken from Table 1. Therefore, for each χ value two tables are provided, one referring to 10x10 X_{eut} and the other to the associated 10x10 T_{eut}, for a total number of 8 tables (Figure S49). The plot of tables can be also saved as image.

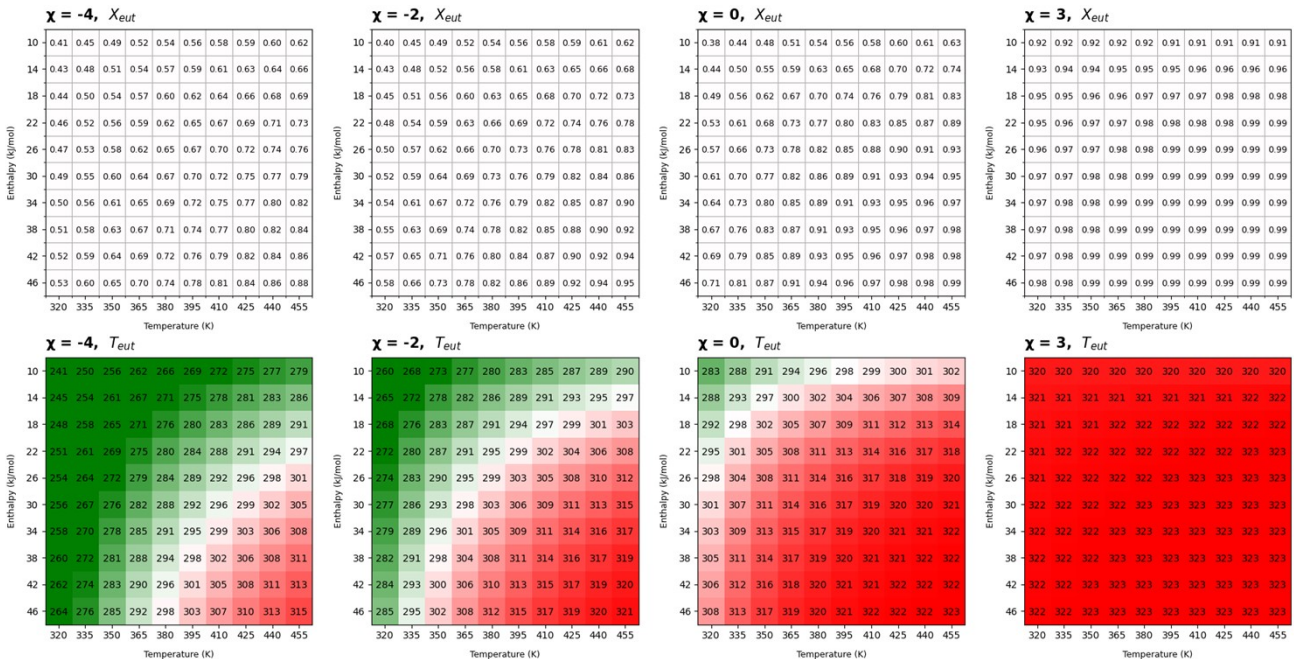

Figure S49. Resuming tables generated by PoEM of eutectic compositions and temperature obtained combining thymol with 10x10 potential coformers at different χ values (-4, -2, 0, 3).

The section of *single-plot* of PoEM's GUI allows to calculate the eutectic point for a binary mixture, starting from the enthalpies of fusion and melting temperatures of both components, and the interaction parameter χ. The Schroeder-Laar's curves of components and the calculated eutectic point are plotted in a binary phase diagram, together with the ideal curves and eutectic point obtained in ideal conditions (χ = 0), to visualize the deviation from ideality (figure S50). Even in this case, the binary phase diagram can be saved as image or CSV file.

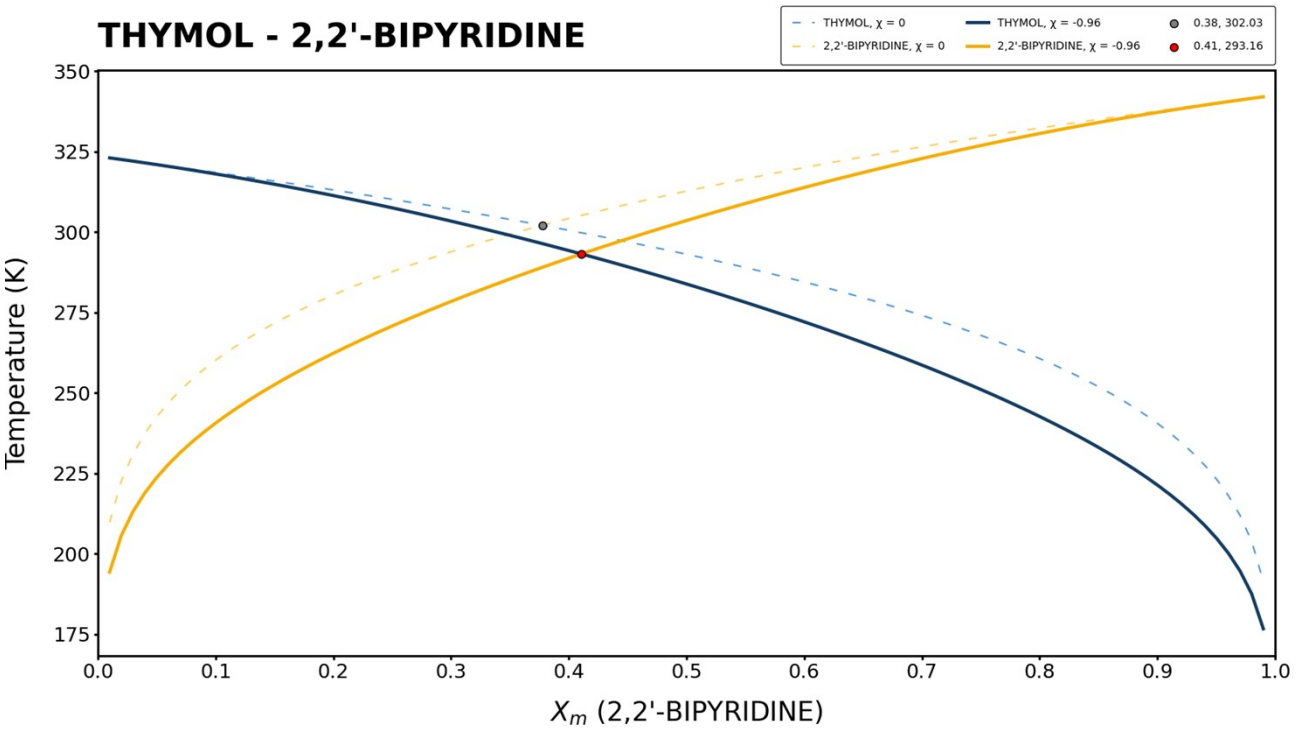

Figure S50. Example of binary phase diagram generated by PoEM for THY-BPY binary mixture in ideal (χ = 0) and not-ideal (χ = - 0.96) conditions.

References

1 J. H. Hildebrand and R. L. Scott, *The Solubility of Non-Electrolytes*, Reinhold Pub. Corp, New York, 1949.

2 P. Virtanen, R. Gommers, T. E. Oliphant, M. Haberland, T. Reddy, D. Cournapeau, E. Burovski, P. Peterson, W. Weckesser, J. Bright, S. J. van der Walt, M. Brett, J. Wilson, K. J. Millman, N. Mayorov, A. R. J. Nelson, E. Jones, R. Kern, E. Larson, C. J. Carey, İ. Polat, Y. Feng, E. W. Moore, J. VanderPlas, D. Laxalde, J. Perktold, R. Cimrman, I. Henriksen, E. A. Quintero, C. R. Harris, A. M. Archibald, A. H. Ribeiro, F. Pedregosa, P. van Mulbregt, A. Vijaykumar, A. Pietro Bardelli, A. Rothberg, A. Hilboll, A. Kloeckner, A. Scopatz, A. Lee, A. Rokem, C. N. Woods, C. Fulton, C. Masson, C. Häggström, C. Fitzgerald, D. A. Nicholson, D. R. Hagen, D. V. Pasechnik, E. Olivetti, E. Martin, E. Wieser, F. Silva, F. Lenders, F. Wilhelm, G. Young, G. A. Price, G. L. Ingold, G. E. Allen, G. R. Lee, H. Audren, I. Probst, J. P. Dietrich, J. Silterra, J. T. Webber, J. Slavič, J. Nothman, J. Buchner, J. Kulick, J. L. Schönberger, J. V. de Miranda Cardoso, J. Reimer, J. Harrington, J. L. C. Rodríguez, J. Nunez-Iglesias, J. Kuczynski, K. Tritz, M. Thoma, M. Newville, M. Kümmerer, M. Bolingbroke, M. Tartre, M. Pak, N. J. Smith, N. Nowaczyk, N. Shebanov, O. Pavlyk, P. A. Brodtkorb, P. Lee, R. T. McGibbon, R. Feldbauer, S. Lewis, S. Tygier, S. Sievert, S. Vigna, S. Peterson, S. More, T. Pudlik, T. Oshima, T. J. Pingel, T. P. Robitaille, T. Spura, T. R. Jones, T. Cera, T. Leslie, T. Zito, T. Krauss, U. Upadhyay, Y. O. Halchenko and Y. Vázquez-Baeza, *Nat. Methods 2020 173*, 2020, **17**, 261–272.

3 M. C. Storer and C. A. Hunter, *Phys. Chem. Chem. Phys.*, 2022, **24**, 18124–18132.

4 M. C. Storer, K. J. Zator, D. P. Reynolds and C. A. Hunter, *Chem. Sci.*, 2023, **15**, 160–170.

5 M. C. Storer and C. A. Hunter, *Chem. Soc. Rev.*, 2022, **51**, 10064–10082.